Table of Contents

From the Editors-in-Chief of the CNS Journal

We are proud to present the first issue of the sixth volume of the Proceedings of the Cognitive Neuroscience Master of the Radboud University. The aim of the Master's programme in Cognitive Neuroscience (CNS) is to prepare students for an interdisciplinary research career. Learning how to publish and effectively communicate research findings is an essential part of this training. Each year, this journal offers students in the CNS programme the opportunity to gain valuable experience in writing, reviewing, editing and publishing. At the same time, the journal allows former CNS students to showcase the results of the internship projects they completed at research institutes and faculties both here in Nijmegen and abroad. The issue you hold in your hands thus reflects the combined efforts of the authors, reviewers, and journal board to create a high-quality, student-run academic journal.

The sixth volume of the journal marks a number of important changes. Firstly, as of this academic year the journal will be published biannually, because a second starting date in February was added to the Master's programme. In order to ensure that articles of the highest quality are published in each issue, this year's web edition will be published together with the second printed edition in June 2011. Secondly, the journal's cover and logo have been redesigned and we are confident that this new layout better reflects the high quality of the articles published in the journal. Thirdly, we would like to invite you to take a look at the updated and expanded journal website. Information about the journal's history and workings are now available and all previous issues can be downloaded and/or ordered online.

In order to maintain the high standards of the student journal, all submitted theses were reviewed by a Master's student and a researcher in the appropriate field. Based on this strict review process, the journal board has selected the best theses for publication in the printed edition. All other theses are available on the journal website (www.ru.nl/master/cns/journal). The four theses you find in this issue address a range of topics from gene-brain structure associations in Alzheimer's Disease to audiovisual integration in Macaques. We hope you will enjoy the articles and gain valuable insights into the diversity of neuroscientific research conducted at Radboud University.

On behalf of the CNS journal board we thank you for your interest in the CNS journal.

Flora Vanlangendonck & Klodiana-Daphne Tona
Editors-in-Chief

From the Director of the
Donders Centre for Cognitive Neuroimaging

Dear readers,

It is a great pleasure for me to contribute this editorial to this, the 6th volume of the CNS journal. When it was originally started this was seen as a highly experimental enterprise with questionable chances of success. However, the journal is flourishing, and this is due entirely to the enthusiasm and expertise of the students of the Master's programme, who have really made this their journal, with each year striving to match and ultimately surpass the achievements of previous years. As a measure of the continuing success, this will be the first year in which two issues will be published: a reflection of the increasing output and high quality of the master's course. Additionally, the cover and logo have been given tremendous new designs.

The Master's course now reflects the four research themes of the Donders Institute with a new track on 'Brain Networks and Neuronal Communication' and much new material to be found under 'Learning, Memory and Plasticity', so in future years we can look forward to a breadth of contributions that matches our four themes. I look forward with great confidence to the development of the journal in coming years and would like to congratulate the editorial staff for a job well done.

With my best wishes,

Prof. Dr. David Norris
Director of the Donders Centre for Cognitive Neuroimaging

Proceedings of the Master's Programme Cognitive Neuroscience of the Radboud University Nijmegen

CR1 genotype is associated with entorhinal cortex volume in young healthy adults

Janita Bralten[1,2]

Supervisors: Barbara Franke[2,3], Alejandro Arias-Vásquez[2,3], Angelien Heister[2], Han G. Brunner[2], Guillén Fernández[1,4], Mark Rijpkema[1]

[1]*Donders Institute for Brain, Cognition and Behavior, Centre for Cognitive Neuroimaging, Radboud University Nijmegen, Nijmegen, The Netherlands*
[2]*Department of Human Genetics, Radboud University Nijmegen Medical Centre, Nijmegen, The Netherlands*
[3]*Department of Psychiatry, Radboud University Nijmegen Medical Centre, Nijmegen, The Netherlands*
[4]*Department of Neurology, Radboud University Nijmegen Medical Centre, Nijmegen, The Netherlands*

Gene-brain structure associations of three recently discovered risk genes for Alzheimer's disease, CLU (rs11136000C>T), CR1 (rs6656401G>A), and PICALM (rs3851179G>A), were investigated in two independent cohorts of young healthy adults (total n=922). We assessed structural differences in two core structures of Alzheimer pathology, entorhinal cortex and hippocampus, by voxel-based morphometry using high-resolution MRI data. For CLU and PICALM no significant genotype-related differences in local gray matter volume were found. CR1 risk allele (A) carriers showed smaller local gray matter volume in the entorhinal cortex. This association, apparent in young healthy adults, might mediate susceptibility for Alzheimer's disease later in life.

Corresponding author: Janita Bralten, Department of Human Genetics (855), Radboud University Nijmegen Medical Centre, PO Box 9101, 6500 HB Nijmegen, The Netherlands, Email: J.Bralten@antrg.umcn.nl

1. Introduction

Late-onset Alzheimer's disease (AD) is among the most common neurodegenerative disorders. AD is a genetically complex disorder (Bertram et al., 2007) influenced by an array of common risk alleles distributed across different genes, affecting a variety of biochemical pathways affecting both the etiology and pathogenesis of AD. APOE contributes strongly to the heritability of AD (Corder et al., 1993), but the search for other genes has been difficult because of the small individual effect sizes of presumed risk genes. Recently, two large genome-wide association studies (GWAS) succeeded in identifying three new genes associated with AD: CLU, CR1, and PICALM (Harold et al., 2009; Lambert et al., 2009). However, the mechanisms behind the increase in AD susceptibility caused by these risk genes remain to be explored.

AD is associated with structural changes in the brain starting with anterior medial temporal lobe atrophy centered in entorhinal cortex and hippocampus (Braak & Braak, 1991; Hyman et al., 1984). For APOE, associations have been found between the risk genotype and entorhinal and hippocampal volume in AD patients (Geroldi et al., 1999), as well as in healthy individuals (Shaw et al, 2007; Wishart et al., 2006). To investigate whether these AD-related brain regions also mediate the effects of the CLU, CR1, and PICALM risk alleles, we studied brain structure in two cohorts of young healthy adults. Structural differences in anterior medial temporal lobe regions, observed already during young adulthood, may contribute to the increased susceptibility for AD later in life.

2. Materials and Methods

2.1 Participants

This study is part of the Brain Imaging Genetics (BIG) project running at the Radboud University Nijmegen (Medical Centre). Saliva and structural MRI data were collected from 922 healthy, highly educated (bachelor student level or higher) adults of Caucasian origin between 18 and 36 years of age, with no self-reported neurological or psychiatric history (for demographics see Table 1). All participants gave written informed consent and the study was approved by the local ethics committee.

2.2 Genotyping

Genetic analyses were performed at the Department of Human Genetics of the Radboud University Nijmegen Medical Centre, in a laboratory which has a quality certification according to CCKL criteria. High molecular weight DNA was isolated from saliva using Oragene containers (DNA Genotek, Ottawa, Ontario, Canada) according to the protocol supplied by the manufacturer.

Affymetrix GeneChip SNP 6.0 arrays (Affymetrix Inc., Santa Clara, CA, USA) were used for genome-wide genotyping of single nucleotide polymorphisms (SNPs) as described before (Franke et al, 2010). Genotypes for SNPs of interest (rs11136000C>T (CLU), rs6656401G>A (CR1), and rs3851179G>A (PICALM)) were selected from these genotyping results for a total of 571 participants (257 in the discovery cohort and 314 in the replication cohort). The remaining participants were genotyped for the three SNPs of interest using Taqman® analysis (assay ID: Taqman assays: CLU: C_11227737_10; reporter 1: VIC-C-allele, forward assay, CR1: C_30033241_10; reporter 1: VIC-A-allele, forward assay, PICALM: C_8748810_10; reporter 1: VIC-C-allele, reverse assay; Applied Biosystems, Nieuwerkerk a/d IJssel, The Netherlands). The APOE genotype was assessed using Taqman® analysis (assay ID: Taqman assays: APOE rs429358: C_3084793_20; reporter 1: VIC-C-allele, reverse assay, APOE rs7412: C_904973_10; reporter 1: VIC-C-allele, reverse assay; Applied Biosystems, Nieuwerkerk a/d IJssel, The Netherlands) and subsequently the two SNP genotypes were combined for confirming the APOE alleles of interest (ε2, ε3 or ε4). Genotyping was carried out in a volume of 10 µl containing 10 ng of genomic DNA, 5 µl of Taqman Mastermix (2×; Applied Biosytems), 0.375 µl of the Taqman assay, and 3.625 µl of Milli-Q. The amplification protocol consisted of an initial denaturation step at 95°C for 10 minutes followed by 40 cycles of denaturation at 92°C for 15 seconds and annealing and extension at 60°C for 60 seconds. Allele-specific fluorescence was subsequently measured on an ABI 7500 FAST (Applied Biosystems). Taqman genotyping assays were validated before use and 5% duplicates and blanks were taken along as quality controls during genotyping. Genotyping results were only considered valid if duplicates and blanks were called correctly and genotypes could be called for at least 95% of the sample tested. Hardy-Weinberg Equilibrium testing was performed on the results.

2.3 MRI acquisition

Magnetic resonance imaging (MRI) data were acquired at the Donders Centre for Cognitive Neuroimaging. All scans covered the entire brain and had a voxel size of 1x1x1 mm³. In the discovery cohort, images were acquired at 1.5 Tesla Siemens Sonata and Avanto scanners (Siemens, Erlangen, Germany), using small variations to a standard T1-weighted 3D MPRAGE sequence (TR 2300 ms, TI 1100 ms, TE 3.03 ms, 192 sagittal slices, field of view 256 mm). These variations included a TR/TI/TE/slices of 2730/1000/2.95/176, 2250/850/2.95/176, 2250/850/3.93/176, 2250/850/3.68/176, and the use of GRAPPA parallel imaging with an acceleration factor of 2. In the replication cohort, images were acquired at 3 Tesla Siemens Trio and TrioTim scanners (Siemens, Erlangen, Germany), using small variations to a standard T1-weighted 3D MPRAGE sequence (TR 2300 ms, TI 1100 ms, TE 3.93 ms, 192 sagittal slices, field of view 256 mm). These variations included a TR/TI/TE/slices of 2300/1100/3.03/192, 2300/1100/2.92/192, 2300/1100/2.96/192, 2300/1100/2.99/192, 1940/1100/3.93/176, 1960/1100/4.58/176, and the use of GRAPPA parallel imaging with an acceleration factor of 2. Slight variations in these imaging parameters have been shown not to affect the reliability of morphometric results (Jovicich et al., 2009).

2.4 Brain segmentation

Raw DICOM MR imaging data were converted to NIFTI format using the conversion as implemented in SPM5 (http://www.fil.ion.ucl.ac.uk/spm/software/spm5/). Normalizing, bias-correcting, and segmenting into gray matter, white matter, and cerebrospinal fluid was performed using the VBM 5.1 toolbox version 1.19 (http://dbm.neuro.uni-jena.de/vbm/) in SPM using priors (default settings). This method uses an optimized VBM protocol (Ashburner et al., 2000, Good et al., 2001) as well as a model based on Hidden Markov Random Fields (HMRF) developed to increase signal-to-noise ratio (Cuadra et al., 2005). Total volume of gray matter, white matter, and cerebrospinal fluid was calculated by adding the resulting tissue probabilities. Total brain volume was defined as the sum of white matter and gray matter volume.

2.5 Voxel-Based Morphometry

Diffeomorphic image registration was performed using the DARTEL toolbox in SPM (Ashburner et al., 2007). First, all images were realigned to templates created from 556 in-house datasets. Second, Jacobian scaled ('modulated') images were calculated and subsequently transformed to MNI space using affine transformation. Finally, all data were smoothed with an 8 mm FWHM Gaussian smoothing kernel. Data analysis was performed in SPM using the gray matter images.

Associations of the three SNPs with brain structure were assessed in separate analyses. After grouping all datasets according to genotype, images with poor quality or artifacts were identified using the outlier analysis routine implemented in the VBM toolbox. Images that showed a deviation of more than 1.5 times the interquartile range from the median were discarded from further analysis.

2.6 Statistical analysis

Statistical analysis was performed using a GLM approach in SPM. A full-factorial ANCOVA was applied using genotype as factor. The participants' sex, age, total brain volume, MRI scanner protocol and APOE genotype (having 0, 1 or 2 ε4 alleles) were added to the model as covariates. F-tests were performed to assess the main effect of genotype, and subsequent t-tests were applied to investigate the direction of the effect. Bilateral entorhinal cortex and hippocampus were defined as regions of interest and a small volume correction (SVC) for these regions was applied using masks obtained from the WFU Pickatlas (http://www.fmri.wfubmc.edu/cms/software). Entorhinal cortex was defined as Brodmann area 28 and 34 together.

Genotypes of CLU and PICALM were investigated using a genotypic model. To account for the relatively low allele frequency of the CR1 risk allele (A), homozygotes and heterozygotes for the A-allele were combined into one group. To limit multiple testing, we decided to test only one genetic model, based on a recent publication by Zhang et al. (2010). Zhang and colleagues performed both an allelic association analysis and a genotype-based analysis for association with AD, and showed for the same SNP in CR1 as studied here (rs6656401), that the AA+AG genotype had the largest effect size with a 2.4-fold increased risk compared with the GG genotype.

Findings in the discovery cohort (n=430) were

subsequently assessed in the replication cohort (n=492). For this, the brain areas where differences in local gray matter volume had been found in the discovery cohort with p(SVC)<0.05 served as regions of interest for the replication cohort. The exact same regions were tested in both cohorts. The same analysis as in the discovery cohort was also applied to the replication cohort, considering replications significant at p(SVC)<0.05.
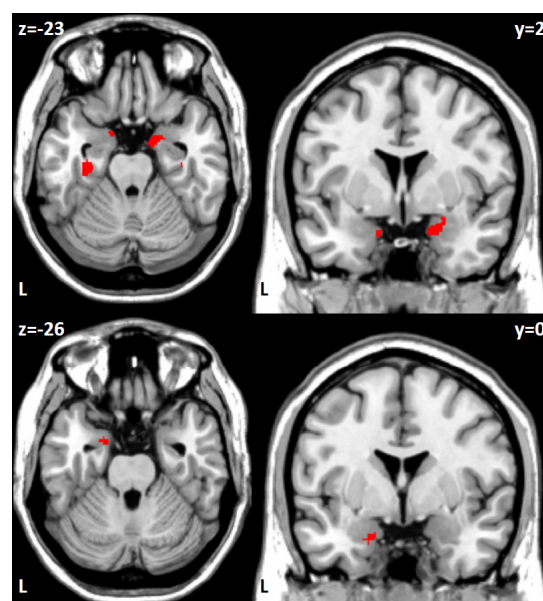
3. Results

The participant demographics and genotype distributions are shown in Table 1. All genotypes were in Hardy-Weinberg Equilibrium (p>0.05). Genotyping was successful in 100%, 97.9%, and 98.3% of the samples for CLU, CR1, and PICALM, respectively.

Table 1. Participant demographics and genotype distributions

Discovery cohort	N	430
	Age (mean)	18-36 (23.3)
	Gender (Female/Male)	223/207
	CLU rs11136000 (CC/CT/TT)	163/207/60
	CR1 rs6656401 (GG/GA/AA)	272/143/14
	PICALM rs3851179 (GG/GA/AA)	143/207/73
Replication cohort	N	492
	Age (mean)	18-36 (22.9)
	Gender (Female/Male)	309/183
	CLU rs11136000 (CC/CT/TT)	182/238/72
	CR1 rs6656401 (GG/GA/AA)	295/165/13
	PICALM rs3851179 (GG/GA/AA)	203/214/66

VBM analysis of local gray matter volume in the entorhinal cortex and the hippocampus showed substantial differences between genotypes. In the discovery cohort associations between CR1 genotype and local gray matter volume were found in the entorhinal cortex (p(SVC)=0.036, maximum at MNI 17,0,-21, Figure 1) and in the hippocampus (p(SVC)=0.012, maximum at MNI -31,-23,-19, Supplementary Figure 1). Carriers of the CR1 rs6656401 A-allele, the risk allele for AD, showed smaller local gray matter volume in these regions compared to GG homozygotes. No statistically significant associations with local gray matter volume were found for CLU or PICALM genotypes

in either entorhinal cortex or hippocampus (all p(SVC)>0.05). To validate the results observed in the discovery cohort, subsequently a VBM analysis was performed in the replication cohort. The association of CR1 genotype with local gray matter volume in the entorhinal cortex was replicated in this independent cohort (p(SVC)=0.031, Figure 1). The findings in the hippocampus were not confirmed in the replication cohort (p(SVC)>0.05).

Fig. 1 Local gray matter volume differences associated with CR1 genotype. Transversal and coronal slices showing smaller gray matter volume (red) in the anterior medial temporal lobe for carriers of the CR1 rs6656401 A-allele in the discovery cohort (top) and in the replication cohort (bottom). Statistical analysis revealed a CR1 association with local gray matter volume in the entorhinal cortex that was replicated in the second cohort. Gray matter volume differences are shown at p(uncorrected) < 0.005 for visualization purposes and projected onto a standard brain in MNI space. Labels are MNI space coordinates. L = left.

4. Discussion

In this study we investigated associations of three recently identified AD risk genes, CLU, CR1, and PICALM, with AD-related brain regions in young healthy adults. Whereas for CLU and PICALM no significant associations with local brain volume were found, carriers of the AD risk allele in CR1 showed smaller local gray matter volume in the entorhinal cortex. This finding was confirmed in a second, independent cohort. The results show that CR1 is associated with structural brain differences already in young healthy adults, and suggest that smaller entorhinal cortex volume may contribute to the increased susceptibility to AD recently found for CR1.

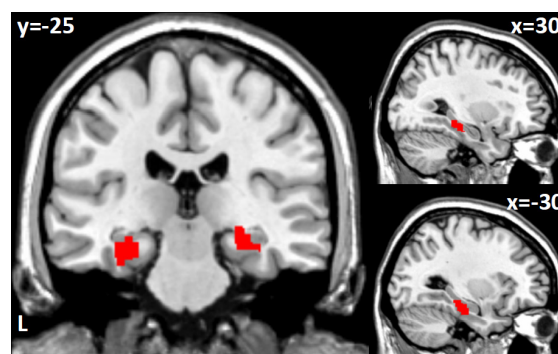The molecular mechanism behind the gene-

AD association for CR1 is largely unknown, although functions in β-amyloid (Aβ) clearance and neuroinflammation have been suggested for this gene (Sleegers et al., 2010). CR1, coding for complement component (3b/4b) receptor 1, may be involved in Aβ clearance through the complement system, which removes pathogens and proteins recognized as foreign. Complement 3b, a product of the complement system, binds to acceptor molecules and mediates subsequent phagocytosis through CR1. Inhibiting complement 3 in mice results in increased Aβ deposition accompanied by neuronal degeneration, supporting a role for the complement system in Aβ clearance (Wyss-Corey et al., 2002). A strong relationship between Aβ deposition and atrophy in a large network of brain areas, including the hippocampus, has been found very early in the disease process of AD (Chetelat et al., 2010). However, whether the role of CR1 in AD susceptibility is mediated through altered Aβ clearance related processes already in young adulthood remains to be investigated.

Our discovery cohort (n=429) is powered to find effect sizes between small and moderate. We recognize that the effect sizes expected in genetic association studies are presumably very small and our initial discovery cohort might not be large enough to find these effects reliably. However, the addition of a replication in an independent cohort strengthens our statistical power substantially. Although combining the two cohorts used in this study will provide increased power, in our case this was not possible, since the data from the two independent cohorts used in this study were recorded using MRI scanners with magnetic field strengths of 1.5T and 3T, respectively. Several studies have shown that combining data of different MRI field strengths in VBM studies may affect region-specific sensitivity and may lead to volume diffence bias (Han et al., 2006; Jovicich et al., 2009; Tardif et al., 2010).

We observed structural brain differences associated with CR1 genotype in young healthy adults. In line with such an early effect on brain structure, Hänggi et al. (Hänggi et al., 2009) found that a common genetic variation in CYP46, a possible risk factor for AD, modulates parahippocampal and hippocampal volumes in a cohort of 81 young adults. In addition, in a large sample of children and adolescents (n=239), Shaw et al. (2007) found reduced cortical thickness in the entorhinal cortex in APOE ε4 carriers compared to non-ε4 carriers. It was proposed that those individuals who have a smaller entorhinal cortex are more readily affected by cortical thinning and pass a critical anatomical

threshold earlier (Shaw et al., 2007). Supporting this, the theory of 'brain reserve capacity' proposes that larger brain volumes provide an individual with more resistance to neuronal degeneration (Mori et al., 1997). Thus, carriers of the AD-risk allele of CR1 may have genetically determined neuroanatomic properties that contribute to an increased susceptibility to neurodegenerative changes occurring later in life.

Although associations of CR1 genotype and grey matter volume of the entorhinal cortex were found, no associations were found for CLU or PICALM genotypes with local volume differences of the entorhinal cortex or the hippocampus. Interpretation of these findings is inconclusive. CLU and PICALM can have no influence on brain volume in line with the current results. The current study might not have the power to find the small effects of CLU and PICALM genotype on these brain volumes, or the effects might not be present at an early age, as only young healthy adults were investigated in the current study, but might be present at later stages in life. Follow-up studies are clearly needed to elucidate the mechanisms of CLU and PICALM further.

Fig.2 Local gray matter volume differences associated with CR1 genotype. Coronal (left) and sagittal (right) slices showing smaller gray matter volume (red) in the anterior medial temporal lobe for carriers of the CR1 rs6656401 A-allele in the discovery cohort. Statistical analysis revealed an association of CR1 genotype with local gray matter volume in the hippocampus (p(SVC) = 0.012), but this could not be confirmed in the replication cohort (p(SVC) > 0.05). Gray matter volume differences are shown at p(uncorrected) < 0.005 for visualization purposes and projected onto a standard brain in MNI space. Labels are MNI space coordinates. L = left.

Entorhinal cortex and hippocampus are the key structures affected early in AD, therefore these were the primary targets for the local gray matter volume analysis in the current study. However, in an exploratory analysis with a statistical threshold of p(uncorrected)<0.005 as shown in Figure 1 and Figure 2, the association of CR1 with brain structure appears not to be confined to these structures, but extends further into the anterior medial temporal

lobe. In the discovery cohort, the gray matter differences found in the hippocampus extend into the collateral sulcus (Figure 1). Furthermore, the amygdala, a brain structure closely linked to both entorhinal cortex and hippocampus and also affected early on in AD (Kromer-Vogt et al., 1990), seems to show reduced local gray matter volume in CR1 A-allele carriers as well. However, these exploratory observations need to be confirmed in follow-up studies.

5. Conclusion

The current study provides the first evidence that CR1 genotype is associated with structural differences in anterior medial temporal lobe regions in young healthy adults. Carriers of the CR1 rs6656401 AD-risk allele show smaller local gray matter volume particularly in the entorhinal cortex, which might contribute to an increased susceptibility for AD later in life.

Acknowledgments

References

Ashburner, J., Friston, K.J., 2000. Voxel based morphometry-the methods. Neuroimage. 11, 805-821.

Ashburner ,J., 2007. A fast diffeomorphic image registration algorithm. Neuroimage. 38, 95-113.

Bertram, L., McQueen, M.B., Mullin, K., Blacker, D., Tanzi, R.E.,2007. Systematic meta-analyses of Alzheimer disease genetic association studies: the AlzGene database. Nat Genet. 39(1), 17-23.

Braak, H., Braak, E., 1991. Neuropathological stageing of Alzheimer-related changes. Acta Neuropathol. 82, 239-259.

Chetelat, G., Villemagne, V.L., Bourgeat, P., Pike, K.E., Jones, G., Ames, D., Ellis, K.A., Szoeke, C., Martins, R.N., O'Keefe, G.J., Salvado, O., Masters, C.L., Rowe, C.C.,2010. Relationship between atrophy and beta-amyloid deposition in Alzheimer disease. Ann Neurol. 67(3), 317-324.

Corder, E.H., Saunders, A.M., Strittmatter, W.J., Schmechel, D.E., Gaskell, P.C., Small, G.W., Roses, A.D., Haines, J.L., Pericak-Vance, M.A., 1993. Gene dose of apolipoprotein E type 4 allele and the risk of Alzheimer's disease in late onset families. Science. 261,921-923.

Cuadra, M.B., Cammoun, L., Butz, T., Cuisenaire, O., Thiran, J.P., 2005. Comparison and validation of tissue modelization and statistical classification methods in T1-weighted MR brain images. IEEE Trans. Med. Imaging. 24, 1548-1565.

Franke, B., Vasquez, A.A., Veltman, J.A., Brunner, H.G., Rijpkema, M., & Fernández, G., 2010. Genetic variation in CACNA1C, a gene associated with bipolar disorder, influences brainstem rather than gray matter volume in healthy individuals. Biol Psychiat. 68(6), 586-588.

Geroldi, C., Pihlajamaki, M., Laakso, M.P., DeCarli, C., Beltramello, A., Bianchetti, A., Soininen, H., Trabucchi, M., Frisoni, G.B., 1999. APOE-epsilon4 is associated with less frontal and more medial temporal lobe atrophy in AD. Neurology. 53(8), 1825-1832.

Good,C.D., Johnsrude, I.S., Ashburner, J., Henson, R.N., Friston, K.J., Frackowiak, R.S., 2001. A voxel-based morphometric study of ageing in 465 normal adult human brains. Neuroimage. 14, 21-36.

Han, X., Jovicich, J., Salat, D., van der Kouwe, A., Quinn, B., Czanner, S., Busa, E., Pacheco, J., Albert, M., Killiany, R., Maguire, P., Rosas, D., Makris, N., Dale, A., Dickerson, B., Fischl, B. 2006. Reliability of MRI-derived measurements of human cerebral cortical thickness: the effects of field strength, scanner upgrade and manufacturer. Neuroimage. 32, 180-194.

Hänggi, J., Mondadori, C.R., Buchmann, A., Henke, K., Hock, C., 2009. A CYP46 T/C SNP modulates parahippocampal and hippocampal morphology in young subjects. Neurobiol Aging, in press.

Harold, D., Abraham, R., Hollingworth, P., Sims, R., Gerrish, A., Hamshere, M.L., Pahwa, J.S., Moskvina, V., Dowzell, K., Williams, A., Jones, N., Thomas, C., Stretton, A., Morgan, A.R., Lovestone, S., Powell, J., Proitsi, P., Lupton, M.K., Brayne, C., Rubinsztein, D.C., Gill, M., Lawlor, B., Lynch, A., Morgan, K., Brown, K.S., Passmore, P.A., Craig, D., McGuinness, B., Todd, S., Holmes, C., Mann, D., Smith, A.D., Love, S., Kehoe, P.G., Hardy, J., Mead, S., Fox, N., Rossor, M., Collinge, J., Maier, W., Jessen, F., Schurmann, B., van den Bussche, H., Heuser, I., Kornhuber, J., Wiltfang, J., Dichgans, M., Frolich, L., Hampel, H., Hull, M., Rujescu, D., Goate, A.M., Kauwe, J.S.,

Cruchaga, C., Nowotny, P., Morris, J.C., Mayo, K., Sleegers, K., Bettens, K., Engelborghs, S., De Deyn, P.P., Van Broeckhoven, C., Livingston, G., Bass, N.J., Gurling, H., McQuillin, A., Gwilliam, R., Deloukas, P., Al-Chalabi, A., Shaw, C.E., Tsolaki, M., Singleton, A.B., Guerreiro, R., Muhleisen, T.W., Nothen, M.M., Moebus, S., Jockel, K.H., Klopp, N., Wichmann, H.E., Carrasquillo, M.M., Pankratz, V.S., Younkin, S.G., Holmans, P.A., O'Donovan, M., Owen, M.J., Williams, J., 2009. Genome-wide association study identifies variants at CLU and PICALM associated with Alzheimer's disease. Nat Genet. 41, 1088-1093.

Hyman, B.T., Van Hoesen, G.W., Damasio, A.R., Barnes, C.L., 1984. Alzheimer's disease: cell-specific pathology isolates the hippocampal formation. Science. 225, 1168-1170.

Jovicich, J., Czanner, S., Han, X. Salat, D., van der Kouwe, A., Quinn, B., Pacheco, J., Albert, M., Killiany, R., Blacker, D., Maguire, P., Rosas, D., Makris, N., Gollub, R., Dale, A., Dickerson, B.C., Fischl, B., 2009. MRI-derived measurements of human subcortical, ventricular and intracranial brain volumes: Reliability effects of scan sessions, acquisition sequences, data analyses, scanner upgrade, scanner vendors and field strengths. Neuroimage. 46, 177-192.

Kromer-Vogt, L.J., Hyman, B.T., Van Hoesen, G.W., Damasio, A.R., 1990. Pathological alterations in the amygdala in Alzheimer's disease. Neurosci. 37, 377-385.

Lambert, J.C., Heath, S., Even, G., Campion, D., Sleegers, K., Hiltunen, M., Combarros, O., Zelenika, D., Bullido, M.J., Tavernier, B., Letenneur, L., Bettens, K., Berr, C., Pasquier, F., Fievet, N., Barberger-Gateau, P., Engelborghs, S., De Deyn, P., Mateo, I., Franck, A., Helisalmi, S., Porcellini, E., Hanon, O., de Pancorbo, M.M., Lendon, C., Dufouil, C., Jaillard, C., Leveillard, T., Alvarez, V., Bosco, P., Mancuso, M., Panza, F., Nacmias, B., Bossu, P., Piccardi, P., Annoni, G., Seripa, D., Galimberti, D., Hannequin, D., Licastro, F., Soininen, H., Ritchie, K., Blanche, H., Dartigues, J.F., Tzourio, C., Gut, I., Van Broeckhoven, C., Alperovitch, A., Lathrop, M., Amouyel, P., 2009. Genome-wide association study identifies variants at CLU and CR1 associated with Alzheimer's disease. Nat Genet. 41, 1094-1099.

Mori, E., Hirono, N., Yamashita, H., Imamura, T., Ikejiri, Y., Ikeda, M., Kitagaki, H., Shimomura, T., Yoneda, Y.,1997. Premorbid brain size as a determinant of reserve capacity against intellectual decline in Alzheimer's disease. Am J Psychiatry. 154(1), 18-24.

Shaw, P., Lerch, J.P., Pruessner, J.C., Taylor, K.N., Rose, A.B., Greenstein, D., Clasen, L., Evans, A., Rapoport, J.L., Giedd, J.N. 2007. Cortical morphology in children and adolescents with different apolipoprotein E gene polymorphisms: an observational study. Lancet Neurol. 6, 494-500.

Shen, Y., Li, R., McGeer, E.G., McGeer, P.L., 1997. Neuronal expression of mRNAs for complement proteins of the classical pathway in Alzheimer brain. Brain Res. 769, 391-395.

Sleegers, K., Lambert, J.C., Bertram, L., Cruts, M., Amouyel, P., Van Broeckhoven, C., 2010. The pursuit of susceptibility genes for Alzheimer's disease: progress and prospects. Trends Genet. 26, 84-93.

Tardif, C.L., Collins, D.L., Pike, G.B., 2010. Regional impact of field strength on voxel-based morphometry results. Hum Brain Mapp. 31,943-957.

Wishart, H.A., Saykin, A.J., McAllister, T.W., Rabin, L.A., McDonald, B.C., Flashman, L.A., Roth, R.M., Mamourian, A.C., Tsongalis, G.J., Rhodes, C.H., 2006. Regional brain atrophy in cognitively intact adults with a single APOE epsilon4 allele. Neurology. 67(7), 1221-1224.

Wyss-Coray, T., Yan, F., Lin, A.H., Lambris, J.D., Alexander, J.J., Quigg, R.J., Masliah, E., 2002. Prominent neurodegeneration and increased plaque formation in complement-inhibited Alzheimer's mice. PNAS. 99, 10837-10842.

Zhang, Q., Yu, J.T., Zhu, Q.X., Zhub, Q., Zhangc, W., Wua, Z., Miaoa, D., Tan, L. 2010. Complement receptor 1 polymorphisms and risk of late-onset Alzheimer's disease. Brain Res. 1348, 216-21.

The ventrolateral prefrontal cortex and the voluntary control of social emotional behaviour: a TMS study

Saskia Koch[1]
Supervisors: Inge Volman[1,2], Ivan Toni[1]

[1] *Donders Institute for Brain Cognition and Behavior, Radboud University Nijmegen, the Netherlands*
[2] *Institute for Psychological Research, Clinical Psychology Unit, Leiden University, the Netherlands*

Previous studies have shown the involvement of the ventrolateral prefrontal cortex (vlPFC) in the voluntary control of social emotional behaviour, as measured with the approach avoidance (AA) task. In this task, both happy and angry faces should be approached or avoided by pulling or pushing a joystick, respectively. Typically, longer reaction times (RTs) and increased error rates are found during affect-incongruent (i.e. approach angry and avoid happy) compared to affect-congruent responses (i.e. approach happy and avoid angry). When making affect- incongruent responses, automatic approach and avoidance tendencies have to be overridden and the opposite actions have to be selected. This study used transcranial magnetic stimulation (TMS) to investigate whether the role of the left vlPFC is crucial during the control of social behaviour. The left vlPFC was inhibited by means of an off-line TMS-protocol (continuous theta burst stimulation; cTBS), in which 600 TMS pulses are applied within 40 seconds. Hereafter, performance on the AA task and a control task (gender evaluation; GE) was assessed. To measure the effect of TMS on regional cerebral blood flow (rCBF) in the stimulated area, arterial spin labelling (ASL) was taken into account. Inhibition of the left vlPFC resulted in decreased performance (i.e. increased error rates) on incongruent trials of the AA task, in which automatic AA tendencies needed to be overruled. When considering the RTs, significant congruency effects (i.e. higher RTs for affect-incongruent compared to affect-congruent responses), but no session-specific effects were found. Furthermore, no congruency or session effects were shown on the GE task, in which implicit emotion evaluations were elicited. Taken together, these results indicate that the left vlPFC is crucial in the voluntary control of social emotional behaviour. Additional ASL data-analysis revealed relative increased rCBF in the left vlPFC compared to left and right V1, but not to the right vlPFC after cTBS stimulation. As both the left and right vlPFC are involved in performance on the AA task, increased rCBF in these areas could indicate a compensatory mechanism to overcome the inhibition of the left vlPFC.

Keywords: continuous theta burst stimulation (cTBS), transcranial magnetic stimulation (TMS), approach avoidance (AA) behaviour, ventrolateral prefrontal cortex (vlPFC), social emotional behaviour, arterial spin labelling (ASL), regional cerebral blood flow (rCBF).

Corresponding author: Saskia Koch, Donders Institute for Brain, Cognition and Behaviour, Radboud University Nijmegen, the Netherlands, saskia.koch@fcdonders.ru.nl

1. Introduction

The human capacity to regulate emotions and control subsequent social emotional behaviour is a highly adaptive and important function of the prefrontal cortex (PFC) (Ochsner & Gross, 2005; Rolls, Hornak, Wade & McGrath, 1994). More specifically, the ventrolateral prefrontal cortex (vlPFC) is found to be important when overriding automatic and motivationally driven response tendencies (Passingham, Toni & Rushworth, 2000). For example, people tend to approach positive and avoid negative facial expressions (Rotteveel and Phaf, 2004). However, when these automatic approach avoidance (AA) tendencies need to be overruled and the opposite actions have to be selected (i.e. approach negative and avoid positive faces), increased BOLD activity has been found in the vlPFC (Roelofs, Minelli, Mars, Van Peer & Toni, 2009; Volman, Toni, Verhagen & Roelofs, submitted). In the abovementioned studies, social AA behaviour has been operationalised by means of the AA task, in which pictures of happy and angry faces should either be approached or avoided by pulling or pushing a joystick, respectively (Rotteveel & Phaf, 2004; Roelofs, Elzinga & Rotteveel, 2005; Heuer, Rinck & Becker, 2007). Typically, both reaction times (RTs) and error rates are found to be higher during the affect-incongruent trials (i.e. approach angry and avoid happy) than during affect-congruent trials (i.e. approach happy and avoid angry) (Rotteveel & Phaf, 2004). That is, when making affect-incongruent responses, automatic tendencies to approach positive and avoid negative facial expressions have to be overridden, resulting in increased RTs and error rates. Furthermore, this congruency effect (i.e. higher RTs and error rates in the incongruent compared to the congruent condition) is present during explicit emotional judgement only, disappearing largely when the judgment is based on an affect-irrelevant dimension, such as gender (Rotteveel & Phaf, 2004). For example, in the gender evaluation (GE) task, in which the decision to either approach or avoid the affective stimulus should be based on its gender, no congruency effect has been found (Rotteveel & Phaf, 2004). Moreover, both Roelofs et al. (2009) and Volman et al. (submitted) found increased activity in the vlPFC during the affect-incongruent trials of the AA task, but not during those of the GE task. Taken together, these findings indicate that the vlPFC is prominently involved in the voluntary selection of emotional actions.

However, the limitation of these previous fMRI studies is that no direct causal relationship can be inferred. Because transcranial magnetic stimulation (TMS) has become an important tool to study causal relationships between brain functioning and behaviour (Pascual-Leone, Walsh & Rothwell, 2000), we used TMS to investigate whether the role of the vlPFC is crucial during the voluntary control of social AA behaviour. More specifically, we inhibited the left vlPFC by means of continuous Theta Burst Stimulation (cTBS; Huang, Edwards, Rounis, Bhatia & Rothwell, 2005). The left vlPFC was chosen as the stimulation site, because it showed higher BOLD activity during affect-incongruent responses than the right vlPFC (Volman et al., submitted). In order to control for the effects of stimulation site, peripheral sensations and the structure of the TMS pulses, two control TMS protocols were used: cTBS stimulation on the vertex and 5-Hz rTMS on the left vlPFC. After application of each TMS-protocol, behavioural performance on both the AA and GE task was assessed. A previous study applying inhibitory repetitive TMS (rTMS) on the dorsal medial prefrontal cortex found decreased performance (i.e. higher error rates) on incongruent trials, in which the direction of an arrow (pointing towards the left or right) should be indicated with the non-matching hand (Taylor, Nobre & Rushworth, 2007). This showed that cTBS stimulation decreased the inhibitory control of the dorsal medial PFC. Significant congruency, but no TMS specific effects were reported on the RTs, indicating that motor responses were not affected (Cho et al., 2009).

To investigate the influence of TMS on regional cerebral blood flow (rCBF) in the stimulated area, arterial spin labelling (ASL) was taken into account. Although the effects of TMS on rCBF have mainly been investigated by means of $H_2^{15}O$-positron emission tomography (PET; Paus et al, 1997, Siebner et al. 2001b), two major disadvantages of PET exist: (1) it suffers from low temporal resolution and (2) the subject is exposed to radioactive substances. By means of ASL, an absolute, quantitative measure of rCBF can be obtained as well (in contrast to BOLD fMRI), but without the disadvantages of PET mentioned above (Moisa, Pohmann, Uludağ, & Thielscher, 2009). Previously, Moisa et al. (2009) not only showed the feasibility of combining TMS with ASL, but also that inhibitory (1Hz) stimulation on the primary motor cortex results in increased rCBF in the stimulated area (Moisa et al., 2009).

Since the left vlPFC has previously been found to be important in the inhibitory control of automatic AA tendencies in favour of other response tendencies

(Roelofs et al., 2009), we hypothesised that its inhibition would result in increased error rates on the affect-incongruent, but not the affect-congruent trials of the AA task. This decreased performance on the affect-incongruent trials would indicate that subjects had more difficulty to override their automatic AA tendencies to approach happy and avoid angry faces. In line with the results of Taylor, Nobre and Rushworth (2007), we hypothesised to find a significant congruency effect concerning the RTs on the AA task, independent of the TMS session. As no consistent congruency effect has been found on the GE task (Roelofs et al., 2009; Volman et al., submitted; Rotteveel & Phaf, 2004) this task was used as a control task. Here, we expected the congruency effect of error rates and RTs to be absent, independent of the specific TMS-protocol applied. Concerning the ASL data, we hypothesised to measure increased rCBF in the stimulated area after inhibition of the left vlPFC, compared to the control stimulations (Moisa et al., 2009).

2. Methods

2.1 Participants

Forty-one right-handed, male participants (aged 18 – 29 years) were invited to take part in the experiment. All participants had normal or corrected-to-normal vision and no history of psychiatric or neurological illness. After having given written informed consent according to the guidelines of the local ethics committee (CMO-Commissie Mensgebonden Onderzoek, region Arnhem-Nijmegen, the Netherlands), they were pre-screened for contra-indications of TMS. In total, seventeen participants dropped out during the experiment, either because they did not find TMS pleasant (thirteen), because of technical problems (one), personal circumstances (two) or because TMS stimulator output exceeded the cut-off threshold (one). Hence, these participants did not complete the experiment. This resulted in 24 subjects for final behavioural analysis. During ASL data analysis, coregistration failed for one participant, resulting in 23 subjects for the functional data analysis. All participants received payment or course credit for their cooperation.
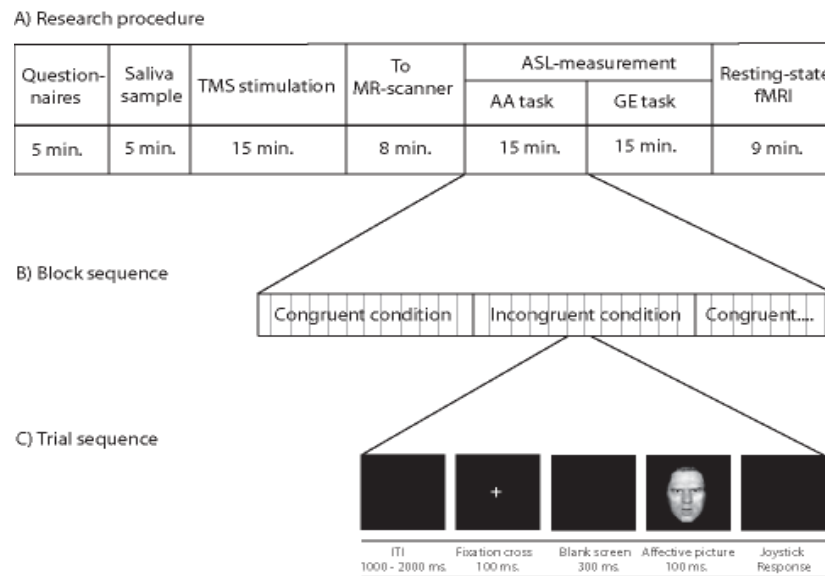
2.2 Procedure and experimental set-up

All participants were invited to four sessions, which were separated by at least one week. The first session was used to pre-screen the subjects for inclusion criteria (e.g. right handedness) and exclusion criteria (i.e. contra-indication for TMS and MRI) and to obtain several baseline measurements. During the three remaining sessions, one of three different TMS-protocols was applied, of which one being the real experimental intervention (i.e. cTBS) and two being control stimulation protocols. Hereafter, performance on the behavioural tasks was assessed.

Upon arrival at the laboratory for the first session, the participants were informed about the experimental procedure and brought to the MR-lab. Here, a structural MR-scan was made and simultaneously a short training of both the AA and the GE task was given. This way, the participants could familiarise with the tasks and the scanning procedure. The structural scan was followed by a baseline resting-state measurement (not used for this report). After completion of several mood-related questionnaires, the participants were brought to the TMS-lab, in which their resting and active Motor Thresholds (rMT and aMT) were determined by means of TMS. In order to get the participants acquainted with TMS, cTBS was administered for 10 seconds at 15% of maximum stimulator output on the left vlPFC and at 80% of aMT on the left vlPFC and vertex.

At the beginning of the three experimental sessions, several mood-related questionnaires were filled in, the participants were reminded about the general procedure of the sessions and were asked whether they had any questions (see figure 1A for the research procedure). After positioning of the earplugs, one of the three different TMS-protocols was applied. Next, the participants were brought to the MR-lab and positioned in the MR-scanner. Communication between the participant and researchers was minimised by giving only the necessary instructions. During the acquisition of ASL, performance on both the AA and GE tasks was assessed. The stimuli of the tasks were presented onto a mirror above the participant's head with a PC running Presentation Software version 10.2 (http://www.neurobs.com). Motor responses were recorded with an MR-compatible joystick (Fiber Optic Joystick, Current Designs), which was placed on the abdomen of the participants, such that comfortable push and pull movements could be executed. Finally, a resting-state measurement was obtained (not used in this report). At the end of the final session, the participants were debriefed about the experiment and asked whether they had any complaints as a result of TMS or MRI.

Fig. 1 (A) Research procedure of the experimental sessions. Each session, a different TMS-protocol (i.e. cTBS, 5Hz and vertex) was applied. **(B)** Block sequence of the AA-task, in which 16 blocks of 12 congruent and incongruent trials were alternated. In the GE-task, the joystick response was based on the gender of the stimulus. **(C)** Sequence of one trial, consisting of an Inter-Trial-Interval (ITI), a fixation cross, a blank screen, the affective picture and a blank screen.

2.2.1 TMS

Transcranial magnetic stimulation (TMS) was applied with a biphasic Magstim Super Rapid Stimulator (The Magstim Company Ltd, Whitland, UK), using a figure-of-eight coil with a diameter of 80 mm. The coil was placed tangentially on the skull and oriented in inferior-superior direction on the left vlPFC and in anterior-posterior direction on the vertex (see Figure 2 for the TMS stimulation sites). During the first session, the resting and active Motor Thresholds (rMT and aMT) of the participants were determined, using a standardised protocol (Rossini et al., 1994). The rMT was defined as the lowest TMS intensity needed to elicit reproducible (i.e. 5 out of 10) and measurable (i.e. peak-to-peak amplitude of at least 50 µV) motor evoked potentials (MEPs) in the first dorsal interosseous (FDI) muscle of the right hand. During the acquisition of the aMT, participants were instructed to maintain FDI muscle contraction by squeezing a tape roll at 10% of their maximal power, which was shown on a screen in front of the participants. The aMT was defined as the lowest TMS stimulator output needed to evoke reproducible (i.e. 5 out of 10) and measurable (i.e. MEPs with peak-to peak amplitude of at least 200 µV) muscle twitches in the activated FDI muscle.

During the three experimental sessions, three different TMS-protocols were applied, one being experimental intervention protocol and two control stimulation protocols. First, to inhibit the left vlPFC, continuous theta burst stimulation (cTBS) was administered on this area. In cTBS, a burst of three pulses at 50Hz is repeated every 200 ms, for a total of 600 pulses (i.e. 40 seconds) (Huang et al., 2005). Previously, it has been shown that cTBS can induce an inhibitory effect of at least 30 minutes when applied on the primary motor cortex and the frontal eye fields (Huang et al., 2005; DiLazzaro et al., 2005; Huble et al., 2008). Secondly, in order to control for the effects of stimulation site, the same cTBS protocol was administered on the vertex. Finally, the other control stimulation consisted of a 5Hz rTMS protocol, which was applied on the site of interest for 40 seconds (i.e. 200 pulses). According to Peinemann et al. (2004), 1800 pulses of 5Hz rTMS applied on the primary motor area induce an excitatory effect that lasts at least 30 minutes. However, 150 pulses did not result in excitation of the motor cortex. Therefore, we assumed that our 5Hz rTMS protocol would not induce an effect, but if any, an excitatory one. By means of this rTMS protocol, we were able to control for both the peripheral sensation of cTBS and the structure of the TMS pulses. That is, one pulse was applied at 5Hz, instead of three pulses applied at 5Hz in the cTBS paradigm. All TMS-protocols were administered at 80 % of aMT (mean stimulation intensity: 29%, SD: 5), with a cut-off threshold of 40% of maximal stimulator output.

In order to position the TMS-coil on the scalp location overlapping the target sites, the T1-weighted MR-scan of each subject was obtained. The MNI (Montreal Neurological Institute)
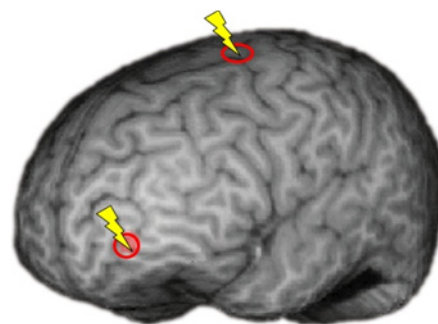
stereotaxic coordinates (-30 58 2), previously reported by Volman et al. (submitted) were used to define a 4 mm sphere on the left vlPFC site. First, the structural MRI-scan was spatially normalised to the standard MNI-space. Hereafter, the inverse parameters of this process were taken to normalise the coordinates of the left vlPFC to the subject space. BrainSight2 (Rogue Research, Montreal, Quebec, Canada) was used to localise the vertex, being defined as the midpoint between nasion and inion, left and right ear and to neuronavigate the TMS-coil on both target sites.

2.2.2 Questionnaires

During the first session, several mood-related questionnaires were filled in: the Beck Depression Inventory (BDI; validated Dutch version: Luteijn & Bouman, 1988), State Trait Anxiety Inventory (STAI-form Y: Spielberger, 1983; validated Dutch version: van der Ploeg, 2000) and the Traumatic Experiences Questionnaire (TEC; validated Dutch version: Vragenlijst naar Belastende Ervaringen (VBE), Nijenhuis, Van der Hart en Vanderlinden, 1995). By means of the BDI and VBE, we could test for the contraindications depression and traumatic experiences, respectively. During the remaining three sessions, the STAI-state was filled in, by which means we could assess the amount of state anxiety.

2.2.3 Behavioural tasks

Following TMS stimulation, both the Approach Avoidance (AA) and the Gender Evaluation (GE) task were administered in counterbalanced order between-subjects within approximately 10 minutes after TMS administration (Mean: 8 min. 15 sec., SD: 1 min. 20 sec). In the two tasks, happy and angry faces (both taken from the same model from a total of 36 models) were displayed at the centre of a black screen. During the AA task, the participants were given written instructions, explicitly asking to evaluate the emotional expression of the face and to make a joystick movement based on that evaluation. In the affect-congruent condition, subjects were instructed to pull the joystick towards their body in response to a happy face (i.e. approach: 'If you see a happy face, pull the joystick towards your body as fast as possible') and to push the joystick away from their body in response to an angry face (i.e. avoidance: 'If you see an angry face, push the joystick away from your body as fast as possible'). During the affect-incongruent condition, the opposite instructions were given (i.e. 'If you see a happy face, push the

Fig. 2 TMS stimulation sites. TMS was applied on the left vlPFC and the vertex.

joystick away from your body as fast as possible' and 'If you see an angry face, pull the joystick towards your body as fast as possible'). In the GE task, the subjects were asked to evaluate the gender of the affective stimulus and to move the joystick based on that evaluation. That is, the subjects were instructed either to pull the joystick towards or away from themselves in response to a male or female face. This resulted in two conditions (i.e. pull-male, push-female and push-male, pull-female). For the pull-male, push-female condition the written instructions given to the participants were: 'If you see a male face, pull the joystick towards your body as fast as possible' and 'If you see a female face, push the joystick away from your body as fast as possible'. The instructions for the other condition were as follows: 'If you see a male face, push the joystick away from your body as fast as possible' and 'If you see a female face, pull the joystick towards your body as fast as possible'. Because the same affective stimuli were used as in the AA task, implicit emotion evaluation was elicited.

As mentioned above, both tasks consisted of two conditions, which were presented in blocks in fully counterbalanced order between- and within-subjects (see Figure 1B for the block sequence of the AA task). At the start of each block, the subjects received written response instructions. During the first session, the subjects performed a training of both tasks, each consisting of 4 blocks of 8 trials and containing models that were not included in the experiment. In the other sessions, each task consisted of 16 blocks of 12 trials. The inter-block interval was varied between 4500 and 5500 ms. All trials started with an inter-trial interval (varied between 1000 and 2000 ms), followed by a fixation point at the centre of the screen (100 ms), a blank screen (300 ms), the affective picture (100 ms) and a blank screen (see Figure 1C for the trial sequence). Joystick responses were valid when the joystick was moved for at least 80% along the sagittal plane and

within 2 seconds after stimulus presentation. Invalid responses were signalled with visual feedback: 'you did not move the joystick far enough'. After each response, the joystick had to be returned to the starting position (i.e. the area between 20% along the sagittal plane) before the end of the inter-trial interval. If not, visual feedback was given: 'return the joystick to the starting position'.

2.2.4 MRI measurements

All MR measurements were obtained with a 1.5 Tesla MRI scanner (Avanto, Siemens Medical Systems, Erlangen, Germany), using a 32-channel head coil. The T1 images were acquired with a MP_RAGE sequence (repetition time (TR) = 2250 ms, echo time (TE) = 2.95 ms, voxel size = 1 x 1 x 1 mm). The continuous ASL data were obtained using a TR of 3500 ms, a TE of 11 ms and with voxel sizes of 3.5 x 3.5 x 5.0 mm.

2.3 Data analysis

2.3.1 Behavioural data

The behavioural data were analysed with SPSS 16 (SPSS Inc., Chicago, IL) and Matlab 7.9 (Mathworks, Natick, MA). First, the joystick movements were kinematically analysed. Correct responses were made when the joystick was moved to the right direction, between 150 and 1500 ms after stimulus presentation, with a peak velocity between 0.1 and 2 cm/second, a movement time between 50 and 400 ms. and within a block in which no more than 50% errors were made. All rejected trials were defined as incorrect responses, except for those trials that were solely rejected because they belonged to a block containing more than 50% errors.

Next, log transformed reaction times (RTs) were calculated for trials in which a correct response was given and averaged per condition (i.e. cTBS – AA task - Congruent). Similarly, the mean log transformed error rates were calculated for each condition. The mean log transformed RTs and error rates in the two control protocols were taken together and averaged as these did not differ significantly per TMS session (for RTs: $t(23)$ = -0.0948, p = 0.353 for congruent and $t(23)$ = -0.680, p = 0.503 for incongruent trials; for error rates: $t(23)$ = 0.029, p = 0.997 for congruent and $t(23)$ = 0.12, p = 0.906 for incongruent trials). A three-way repeated measures MANOVA was conducted on mean log transformed RTs and error rates with Session (cTBS and control),

Task (AA and GE task) and Congruency (Congruent and Incongruent) as factors. Additionally, several covariates, such as stimulator output, session order, task order and mean scores on the STAI questionnaires per session (all Z-transformed) were taken into account in the three-way (Session x Task x Congruency) MANOVA. A four-way (Session x Task x Congruency x Affect) MANOVA was conducted on mean log transformed RTs and error rates, to look at the effects of emotional valence. The α-level was set at p < 0.05 for all analyses.

2.3.2 fMRI data

The continuous ASL-data were analysed with SPM5 (Statistical Parametric Mapping; http://fil.ion.ucl.ac. uk/spm). At the single-subject level, the data were first spatially realigned using six rigid body transformations (i.e. translation and rotation). No consistent motion artefacts were found as a result of joystick movements. After coregistration of the images to the individual's structural T1, spatial smoothing was performed by means of an isotropic 8 mm full-width at half-maximum (FWHM) Gaussian kernel. Because coregistration failed for one subject, the subsequent ASL data analysis was performed on 23 subjects. Next, the CBF-images were reconstructed using the ASL-toolbox of Wang et al. (2008), adapted by Shoazheng Qin (2009) for use at the Donders Centre for Cognitive Neuroimaging (DCCN). In ASL, perfusion images are obtained by pair-wise subtraction of a tag image, in which inflowing blood is magnetically labelled from a control image (Wang et al. 2008). These perfusion images can then be used to obtain a quantitative measure of CBF, expressed in ml/min/100 gram tissue. The CBF-value was calculated after spatial smoothing to reduce CBF signal outliers and before spatial normalization to obtain an unbiased estimate of the CBF value (Wang et al., 2008).

After normalization of the CBF-images to the standard MNI space, mean CBF values were calculated for each of the three sessions for the left and right vlPFC (±30 58 2) and the left and right V1 (±24 -95 -6; Mechelli, Friston, Frackowiak & Price, 2005) with as sphere of 4 mm. Again, the CBF values of the two control sessions were taken together, as these were not significantly different ($t(22)$ = 0.318, p = 0.754 and $t(22)$ = 0.821, p = 0.421 for left and right vlPFC; $t(22)$ = 0.658, p = 0.658 and $t(22)$ = 1.171, p = 0.254 for left and right V1). This resulted in one CBF value for the control conditions per site. In order to correct for session specific rCBF

Table 1. Reaction times (in ms) and error rates (in percentage) (mean ± SEM) per TMS-session (cTBS and control) for congruent and incongruent responses towards happy and angry faces in the AA and GE task.

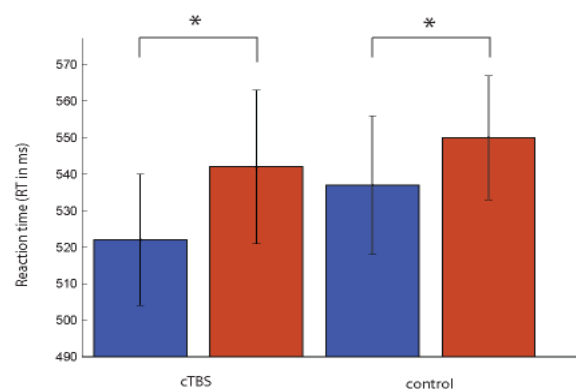|		AA		GE	
		cTBS	control	cTBS	control
Reaction times (in ms)					
Congruent	Happy	498 ± 16	511 ± 18	529 ± 18	547 ± 19
	Angry	548 ± 20	564 ± 20	549 ± 22	554 ± 19
Incongruent	Happy	550 ± 22	561 ± 19	510 ± 18	533 ± 16
	Angry	535 ± 21	540 ± 16	534 ± 20	552 ± 17
Error rates (in percentage)					
Congruent	Happy	4.20 ± 0.72	5.82 ± 1.01	9.56 ± 1.43	9.07 ± 1.24
	Angry	6.35 ± 0.88	7.86 ± 1.09	11.89 ± 1.40	13.63 ± 1.48
Incongruent	Happy	13.63 ± 1.89	10.72 ± 0.95	10.42 ± 1.56	8.51 ± 0.91
	Angry	11.42 ± 1.80	7.12 ± 0.90	12.50 ± 1.93	12.24 ± 1.47

differences, relative change in rCBF in the left vlPFC compared to each of the three control sites was calculated. A one-way repeated measures ANOVA was conducted on relative change in CBF value with Session (cTBS and control) as factor. Additionally, several covariates, such as session order, task order, STAI scores per condition and stimulator output (all Z-transformed) were taken into account. Next, the difference between relative rCBF in the cTBS session and in the control sessions was calculated and correlated with the significant covariate(s). The α-level was set at $p < 0.05$
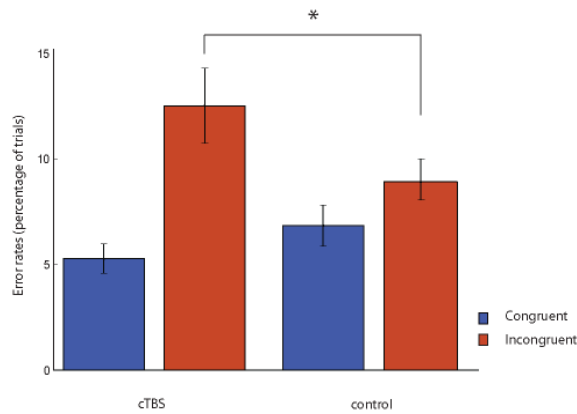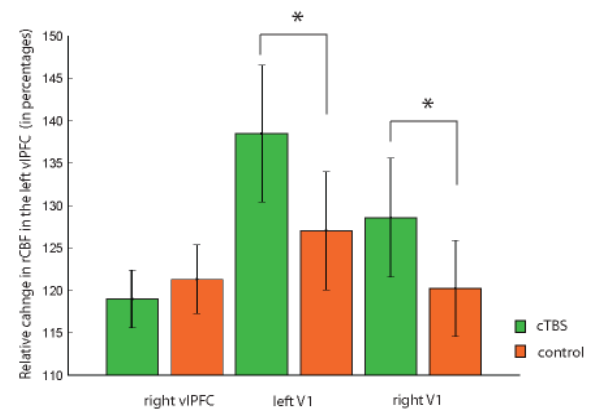
3. Results

3.1 Behavioural results

Mean RTs in ms and error rates in percentage are presented in Table 1. The three-way (Session x Task x Congruency) repeated measures MANOVA on RTs and error rates showed a significant main effect of Congruency ($F_{(2, 22)} = 3.829$, $p = 0.037$), a significant Session x Congruency interaction ($F_{(2, 22)} = 3.938$, $p = 0.037$) and a significant Task x Congruency interaction ($F_{(2, 22)} = 7.513$, $p = 0.003$). The univariate tests indicated that Session x Congruency interaction was significant for error rates ($F_{(1)} = 7.642$, $p = 0.011$), while the Task x Congruency interaction was present for both RTs ($F_{(1)} = 15.063$, $p = 0.001$) and error rates ($F_{(1)} = 8.497$, $p = 0.008$). The main effect of Congruency was found to be significant for error rates only ($F_{(1)} = 7.9$, $p = 0.01$). Although no Session x Task x Congruency interaction was found, the repeated measures MANOVA was performed separately

for the AA- and GE tasks. Previous studies have repeatedly shown both tasks to elicit different response tendencies, with the congruency effect being present in the AA task and absent in the GE task (Rotteveel and Phaf, 2004; Roelofs et al., 2009; Volman et al., submitted). When considering the AA task, the two-way (Session x Congruency) repeated measures MANOVA yielded a significant main effect of Congruency ($F_{(2, 22)} = 7.58$, $p = 0.003$) and a Session x Congruency interaction ($F_{(2, 22)} = 4.006$, $p = 0.033$). The univariate tests showed that the Congruency x Session interaction was significant for error rates only ($F_{(1)} = 8.356$, $p = 0.008$), while the main effect of Congruency was present for both RTs ($F_{(1)} = 13.056$, $p = 0.001$) and error rates ($F_{(1)} = 8.853$, $p = 0.007$) (See Figure 3 for the congruency effect on RTs). The reaction times and amount of errors on the AA task were significantly higher during the incongruent than the congruent trials, irrespective of the specific TMS protocol applied.

Fig. 3 Reaction times in ms (mean ± SEM) per TMS-session (cTBS and control) per affect-congruent and affect-incongruent response condition of the AA-task. A significant congruency effect was found in both TMS-sessions.

Fig. 4 Error rates in percentage (mean ± SEM) per TMS-session (cTBS and control) per affect-congruent and affect incongruent condition of the AA task. The errorrates are significantly increased in the incongruent condition of the AA task after cTBS, compared to control stimulation.

Fig. 5 Relative increase in rCBF (mean ± SEM) in the left vlPFC compared to the right vlPFC, left and right V1 per TMS-session (cTBS and control). Relative increase in rCBF value in the left vlPFC compared to both the left and right V1 is higher after cTBS compared to control stimulation. No session specific-effects were found on the left vlPFC – right vlPFC comparison.

When looking into the congruent and incongruent conditions separately, a significant main effect of Session for the incongruent ($F_{(2, 22)}$ = 4.569, p = 0.022), but not for the congruent condition ($F_{(2, 22)}$ = 1.932, p = 0.169) was shown. The effect of Session on the incongruent condition was found to be significant for error rates ($F_{(1)}$ = 6.730, p = 0.016), indicating significantly more errors during the incongruent condition in the cTBS session, compared to the control sessions (see Figure 4 for Session x Congruency effect on the error rates). When considering the GE task, the two-way (Session x Congruency) repeated measures MANOVA on RTs and error rates yielded no significant effects. Additional analysis incorporating the STAI-score for the cTBS and control sessions as covariate, showed no significant results, indicating that the amount of anxiety during the sessions did not influence the behavioural effects mentioned above.

In order to look at possible effects of emotional valence on the Session x Congruency interaction, a four-way (Session x Task x Congruency x Affect) repeated measures MANOVA was conducted. All effects mentioned above remained significant. When considering the AA task, the MANOVA yielded a significant main effect of Affect ($F_{(2, 22)}$ = 5.137, p = 0.015) and a significant Congruency x Affect interaction ($F_{(2, 22)}$ = 33.432, p = 0.0001). However, the Session x Congruency x Affect interaction did not reach significance ($F_{(2, 22)}$ = 0.323, p = 0.727), indicating that the Session x Congruency interaction was not influenced by the emotional valence of the stimulus. The main effect of Affect was found to be significant for RTs only ($F_{(1)}$ = 10.386, p = 0.004), while the Congruency x Affect interaction

showed significance for both RTs ($F_{(1)}$ = 50.5, p = 0.0001) and error rates ($F_{(1)}$ = 33.515, p = 0.0001). When considering the RTs, the Congruency x Affect interaction was shown to result from the effect of movement direction, as pushing the joystick was found to take longer than pulling it, irrespective of congruency. Concerning the error rates, it was shown that congruent responses towards happy compared to angry faces resulted in fewer errors. The reverse was shown for incongruent responses (i.e. fewer errors for incongruent responses towards angry compared to happy faces). The Congruency effect was still present for error rates. When looking at the GE task, the MANOVA yielded a significant main effect of Affect ($F_{(2, 22)}$ = 28.80, p = 0.0001), a significant Session x Affect interaction ($F_{(2, 22)}$ = 4.758, p = 0.019) and a significant Congruency x Affect interaction ($F_{(2, 22)}$ = 5.454, p = 0.012). The univariate statistics showed that the main effect of Affect was present for both RTs ($F_{(1)}$ = 42.903, p = 0.0001) and error rates ($F_{(1)}$ = 22.275, p = 0.0001). The Session x Affect interaction was found to be significant for incorrect answers only ($F_{(1)}$ = 5.021, p = 0.035), showing more errors towards happy but fewer towards angry faces in the cTBS, compared to the control session. The Congruency x Affect interaction was significant for RTs only ($F_{(1)}$ = 8.119, p = 0.009), indicating that responses towards angry faces take longer than towards happy faces.

3.2 Functional MRI results

The mean relative change in rCBF values in the left vlPFC compared to the three control areas (i.e. right vlPFC and left and right V1) are presented in

Table 2. Relative change in CBF value in left vlPFC compared to the right vlPFC, left V1 and right V1 per TMS-session (cTBS and control).

	cTBS	control
Relative change in CBF in left vlPFC		
right vlPFC	118.97 ± 3.39	121.32 ± 4.04
left V1	138.48 ± 8.04	127.04 ± 6.97
right V1	128.59 ± 7.01	120.25 ± 5.65

Table 2. A one-way (Session) repeated measures ANOVA was conducted on the relative change in rCBF value. A significant session effect was found for left vlPFC – left V1 (F(1) = 9.723, p = 0.03) and for left vlPFC – right V1 (F(1) = 5.365, p = 0.03). These results indicated that the increased rCBF in the left vlPFC compared to both the left and right V1, is higher after cTBS than after the control stimulations (see Figure 5). When conducting the same one-way (Session) repeated measures ANOVA on the relative rCBF change for left vlPFC – right vlPFC, no significant main effect of Session was found (F(1) = 0.421, p = 0.523).

The covariates Session Order and Stimulator Output interacted significantly in the effect of Session on rCBF for left vlPFC – right V1 (F(1) = 7.151, p = 0.014 and F(1) = 7.474, p = 0.012, respectively). Both covariates correlated positively with the difference in relative rCBF between cTBS and control stimulation (r = 0.451, p = 0.031 for Session Order and r = 0.631, p = 0.001 for Stimulator Output). This indicated that relative rCBF in the left vlPFC after cTBS stimulation increased as a function of Stimulator output and Session order. When looking at rCBF in the left vlPFC compared to the left V1, both Session Order and Stimulator Output showed a non-significant trend (F(1) = 3.996, p = 0.059 and F(1) = 4.0880, p = 0.056, respectively). Furthermore, these covariates influenced the difference in relative rCBF value between cTBS and control session in the same direction as on the right V1 (r = 0.4, p = 0.059 for Stimulator output and r = 0.234, p = 0.28 for Session Order). An association between the rCBF measures and the behavioural effects did not yield significant results.

4. Discussion

This study aimed at identifying a causal relationship between left ventrolateral prefrontal (vlPFC) functioning and the voluntary control of social emotional behaviour, as measured with the approach avoidance (AA) task. Inhibition of the left vlPFC by means of continuous theta burst stimulation (cTBS; Huang et al., 2005) resulted in decreased performance (i.e. higher error rates) on the affect-incongruent condition of the AA task. When considering the reaction times (RTs), significant congruency effects (i.e. higher RTs for affect-incongruent compared to affect-congruent responses) but no session-specific effects were found. Furthermore, no congruency or session effects were shown on the gender evaluation (GE) task, in which only implicit emotion evaluations were elicited. Additional fMRI data-analysis (i.e. arterial spin labelling; ASL) revealed relative increased regional cerebral blood flow (rCBF) in the left vlPFC as a result of cTBS stimulation.

Crucially, the behavioural effect of increased error rates after cTBS stimulation was limited to the affect-incongruent condition of the AA task, being absent in the GE task and in the affect-congruent condition of the AA task. Moreover, the absence of session-specific effects on RTs in both the AA and GE tasks indicates that cTBS stimulation did not change motor performance per se (Cho et al., 2009). Rather, the left vlPFC seems to be crucial in inhibiting automatic response tendencies towards emotional stimuli in favour of other stimulus-response combinations (Roelofs et al., 2009). More generally, by 'accessing and maintaining goal-relevant information for the control of action' (Souza, Donuhue & Bunge, 2009, p.299) this area seems to select rule-driven response tendencies in favour of more automated responses (Thompson-Schill, Bedney & Goldberg, 2005). Therefore, we argue that inhibition of the left vlPFC leads to increased difficulty to override automatic response tendencies in favour of rule-driven responses and, as a consequence, in increased error rates when rule-driven (e.g. affect-incongruent) responses should be made. Given the absence of congruency effects on the GE task, it could be argued that the automatic AA response tendencies are not initiated when the affective stimulus is processed unconsciously (Rotteveel and Phaf, 2004). In the GE task, the decision to pull or push the joystick should be based on the gender of the affective stimulus, eliciting implicit emotion evaluations only. As the initiation of motivationally driven AA tendencies seems to

depend on the conscious and explicit evaluation of the affective stimulus, our results highlight the importance of the left vlPFC in the voluntary control of social AA behaviour (Rotteveel & Phaf, 2004; Roelofs et al., 2009).

ASL data-analysis revealed increased relative rCBF in the cTBS stimulated area, relative to the left and right occipital cortex, but not to the right vlPFC. Furthermore, this effect was found to be positively related to the amount of stimulator output. As both the left and right vlPFC are known to be important during performance on the AA task (Volman et al., submitted), rCBF could be increased in these areas to compensate for the inhibition of the left vlPFC. To our knowledge, the physiological effects of cTBS stimulation on cerebral blood flow, as measured with ASL, have never been investigated before. Previous inhibitory (i.e.1Hz) rTMS studies targeting the primary motor and/or somatosensory cortices, reported increased rCBF in the targeted sites as well, being positively related to stimulation intensity (PET data: Speer et al., 2003a and Siebner et al., 2001, ASL-data: Moisa et al., 2009). However, whether these physiological effects could be extended to the PFC, remains subject to debate (Speer et al, 2003b). For example, Nahas et al. (2001) found that left prefrontal stimulation (i.e.1Hz rTMS) at 100% and 120% of MT increased activation patterns (as measured with BOLD fMRI) in both the stimulated site and its contralateral counterpart. When applying the same rTMS stimulation at 80% of MT on the left PFC, increased rCBF was measured in the anterior cingulate cortex but not in the PFC. In contrast to the abovementioned findings, Huble et al. (2008) measured decreased BOLD activity patterns 20 to 35 minutes after cTBS stimulation on the left frontal eye fields (FEF). Also, the study of Speer et al. (2003b) reported decreased rCBF (as measured with PET) in the 1Hz rTMS stimulated PFC, being positively related to stimulator output (i.e. higher stimulator output resulting in less rCBF).

One important issue concerning off-line TMS-studies is the duration of the TMS effect. This issue is especially relevant when considering the fact that the effects of TMS stimulation could be different depending on the site of stimulation (e.g. Kähkönen, Wilenius, Komssi & Ilmoniemi, 2004; Kähkönen, Komssi, Wilenius & Ilmoniemi, 2005). Previously, it has been shown that cTBS induces an inhibitory effect of at least 30 minutes when applied on the primary motor cortex (Huang et al., 2005), on the dorsal premotor cortex (Huang et al, 2009) and on the frontal eye fields (FEF) (Nyffeler et al., 2006; Huble et al., 2008). Furthermore, it has been shown

that cTBS induces an inhibitory effect when applied on the primary visual (Franca, Koch, Mochizuki, Huang & Rothwell, 2006) and somatosensory cortex (Ishikawa et al., 2007), although the effect on the somatosensory cortex lasted for 13 minutes only. In our study, task performance and ASL measurement were started within 10 minutes and finished within 35 minutes after cTBS stimulation. Although this report did not look into the time course of rCBF, results of the study of Huble et al. (2008) indicated that the effect of cTBS stimulation on the FEF reached significance compared to baseline at 20 to 35 minutes after stimulation, disappearing largely after 60 minutes (Huble et al., 2008). Therefore, the tasks in our study were likely to be administered within the time window of the TMS effect.

This study suffers from several limitations. As mentioned above, this report did not look into the time course of the ASL-measurement. Given the unknown duration of the cTBS effect on the left vlPFC, we could have gained valuable information by this. Furthermore, when analysing the ASL data, mean rCBF values in the left vlPFC were compared to the right vlPFC and to the left and right occipital lobe. However, given the fact that rTMS affects both local and remote areas (Huble et al., 2008), additional analyses at the second level should still be performed, allowing us to look at stimulation effects at the whole-brain level. A second limitation is that no hormonal measurements were taken into account. Especially considering that cortisol and testosterone are known to modulate the control of social emotional behaviour (Volman et al., submitted) and HPA-axis response is implicated in the physiological effects of rTMS (Baeken, Vanderhasselt & Raedt, in press). Finally, only males participated in our study. Previous studies on the control of social emotional behaviour and its neural correlates focussed on male participants as well (Roelofs et al, 2009, Volman et al., submitted). As a result, however, we are not able to generalise our results to women, especially when considering the modulatory effects of hormones, such as testosterone, on the regulation of social behaviour (Volman et al., submitted).

Future TMS studies could be aimed at targeting the right vlPFC, as this site has been shown that to be involved during the control of social emotional behaviour as well (Volman et al., submitted). This way, valuable insights into the differences and similarities of left and right prefrontal functioning and the control of social emotional behaviour could be gained. Also, future research could be aimed at identifying the neural correlates of social AA behaviour in female participants. This seems

especially important when considering the fact that SAD, in which social emotional behaviour and PFC functioning are found to be disturbed is more prevalent among females than males. Therefore, new research on the functioning of the prefrontal cortex and the control of social emotional behaviour in females could be of great clinical importance.

5. Conclusion

In sum, this study showed the importance of the left vlPFC in the voluntary control of social emotional behaviour. That is, inhibition of the left vlPFC resulted in decreased performance of affect-incongruent responses, during which automatic response tendencies need to be overridden in favour of rule-driven responses. This study provided new insights into social emotional behaviour and the normal functioning of the PFC. Our fMRI results indicate that cTBS stimulation on the left vlPFC leads to increased rCBF in the stimulated area. As both the left and right vlPFC are involved in performance on the AA task, increased rCBF in these areas could indicate a compensatory mechanism to overcome the inhibition of the left vlPFC.

Acknowledgements

References

Baeken, C., Vanderhasselt, M.A. & De Raedt, R. (in press). Baseline 'state anxiety' influences HPA-axis sensitivity to one sham-controlled HF-rTMS session applied to the right dorsolateral prefrontal cortex. Psychoneuroendocrinology. doi:10.1016/j.psyneuen.2010.06.006

Cho, S.S., Ko, J.H., Pellecchia, G., Eimeren, T. van, Cilia R. & Strafella, A.P. (2010). Continuous theta burst stimulation of right dorsolateral prefrontal cortex induces changes in impulsivity level. Brain Stimulation, 3(3), 170-176. doi:10.1016/j.brs.2009.10.002

Di Lazzaro, V., Pilato, F., Saturno, E., Oliviero, A., Dileone, M., Mazzone, P., Insola, A., Tonali, P.A., Ranieri, F. Huang, Y.Z.,& Rothwell J.C. (2005). Theta-burst repetitive transcranial magnetic stimulation suppresses specific excitatory circuits in the human motor cortex. Journal of Physiology, 565.3, 945-950.

doi: 10.1113/jphysiol.2005.087288

Franca, M., Koch, G., Mochizuki, H., Huang Y.Z., & Rothwell, J.C. (2006). Effects of theta burst stimulation protocols on phosphene threshold. Clinical Neurophysiology, 117, 1808–1813. doi:10.1016/j.clinph.2006.03.019

Heuer, K., Rinck, M. & Becker, E.S. (2007). Avoidance of emotional facial expressions in social anxiety: the approach-avoidance task. Behaviour Resech Therapy, 45(12), 2990–3001. doi:10.1016/j.brat.2007.08.010

Huang, Y.Z., Edwards, M.J., Rounis, E., Bhatia, K.P. & Rothwell, J.C. (2005). Theta burst stimulation of the human motor cortex. Neuron, 54, 201-206. doi:10.1016/j.neuron.2004.12.033

Huble, D., Nyffelerm T., Wurtz, P., Chaves, S., Pflugschaupt, T., Lüthl, M. Von Wartburg, R., Wiest, R., Dierks, T., Strik, W.K., Hess, C.W. & Müri, R.M. (2008). Time course of blood oxygenation level dependent signal response after theta burst transcranial magnetic stimulation of the frontal eye fields. Neuroscience, 151, 921–928. doi:10.1016/j.neuroscience.2007.10.049

Ishikawa, S. Matsunaga, K., Nakanishi, R. Kawahira, K., Murayama, N., Tsuji, S., Huang. Y-Z. & Rothwell, R.C. (2007). Effect of theta burst stimulation over the human sensorimotor cortex on motor and somatosensory evoked potentials. Clinical Neurophysiology, 118, 1033–1043. doi:10.1016/j.clinph.2007.02.003

Kähkönen, S., Wilenius, J., Komssi, S. & Ilmoniemi, R.J. (2004). Distinct differences in cortical reactivity of motor and prefrontal cortices to magnetic stimulation. Clinical Neurophysiology, 115, 583-588. doi:10.1016/j.clinph.2003.10.032

Kähkönen, S., Komssi, S., Wilenius, J. & Ilmoniemi, R.J. (2005). Prefrontal TMS produces smaller EEG responses than motor-cortex TMS: implications for rTMS treatment in depression. Psychopharmacology, 181, 16–20. doi: 10.1007/s00213-005-2197-3

Luteijn, F. and Bouman, T. K. (1988). The Concepts of Depression, Anxiety, and Neuroticism in Questionnaires. European Journal of Personality, 2, 113-20.

Mechelli, A., Friston, K.J., Frackowiak, R.S. & Price, C.J. (2005). Structural Covariance in the Human Cortex. The Journal of Neuroscience, 25(36), 8303– 8310. doi:10.1523/JNEUROSCI.0357-05.2005

Moisa, M., Pohmann, R., Uludağ, K. & Thielscher, A. (2009). Interleaved TMS/CASL: Comparison of different rTMS protocols. NeuroImage, 49, 612 – 620. doi:10.1016/j.neuroimage.2009.07.010

Nahas, Z., Lomarev, M., Roberts, D.R., Shastri, A., Lorberbaum, J.P., Teneback, C., McConnell, K., Vincent, D.J., Li, X., George, M.S. & Bohning, D.E. (2001). Unilateral Left Prefrontal Transcranial Magnetic Stimulation (TMS) Produces Intensity-Dependent Bilateral Effects as Measured by Interleaved BOLD fMRI. Biological Psychiatry, 50, 712 – 720. doi:10.1016/S0006-3223(01)01199-4

Nyffeler, T., Wurtz, P., Lüscher, H-R., Hess, C.W., Senn, W. Pflugshaupt, T., Von Wartburg, R., Lüthi, M. & Mür, R.M. (2006). Extending lifetime of plastic changes in the human brain. European Journal of Neuroscience, 24, 2961–2966. doi: 10.1111/j.1460-9568.2006.05154.x

Ochsner, K.N. & Gross, J.J. (2005). The cognitive control of emotion. Trends in Cognitive Sciences, 9(5), 242–9. doi:10.1016/j.tics.2005.03.010

Pascual-Leone, A., Walsh, V. & Rothwell, J. (2000). Transcranial magnetic stimulation in cognitive neuroscience - virtual lesion, chronometry and functional connectivity. Current opinion in neurobiology, 10, 232-237. doi:10.1016/S0959-4388(00)00081-7

Passingham, R.E., Toni & I., Rushworth, M.F. (2000). Specialisation within the prefrontal cortex: the ventral prefrontal cortex and associative learning. Experimental Brain Research, 133(1), 103–13. doi: 10.1007/s002210000405

Paus, T., Jech, R., Thompson, C.J., Comeau, R., Peters, T. & Evans, A.C., (1997). Transcranial Magnetic Stimulation during positron emission tomography: a new method for studying connectivity of the human cerebral cortex. Journal of Neuroscience, 17, 3178–3184. Http://www.jneurosci.org/cgi/content/full/17/9/3178

Peinemann, A., Reimer, B., Löer, C., Quartarone, A., Münchau, A., Conrad, B. & Siebner, H. N. (2004). Long-lasting increase in corticospinal excitability after 1800 pulses of subthreshold 5Hz repetitive TMS to the primary motor threshold. Clinical neurophysiology, 115, 1519-1526.

Roelofs, K., Minelli, A., Mars, R.B., Van Peer, J. & Toni, I. (2009). On the neural control of social emotional behavior. SCAN, 4, 50-58. doi:10.1016/j.psyneuen.2005.02.008

Rolls, E.T., Hornak, J., Wade, D. & McGrath, J. (1994). Emotion-related learning in patients with social and emotional changes associated with frontal lobe damage. Journal of Neurology, Neurosurgery, and Psychiatry, 57, 1518–24. doi:10.1136/jnnp.57.12.1518

Rossini et al. (1994). Non-invasive electrical and magnetic stimulation of the brain, spinal cord and roots: basic principles and procedures for routine clinical application. Report of an IFCN committee. Electroencephalography and clinical neurophysiology, 91, 79-92.

Rotteveel, M. & Phaf, R.H. (2004). Automatic affective evaluation does not automatically predispose for arm flexion and extension. Emotion, 4(2), 156–72.doi: 10.1037/1528-3542.4.2.156

Siebner, H.R., Takano, B., Peinemann, A., Schwaiger, M., Conrad, B., Drzezga, A., (2001). Continuous Transcranial Magnetic Stimulation during positron emission tomography: a suitable tool for imaging regional excitability of the human cortex. NeuroImage, 14, 883–890. doi:10.1006/nimg.2001.0889

Souza, M.J., Donohue, S.E. & Bunge, S.A. (2009).

Controlled retrieval and selection of action-relevant knowledge mediated by partially overlapping regions in left ventrolateral prefrontal cortex. NeuroImage, 46(1), 299- 307. doi:10.1016/j.neuroimage.2009.01.046

Speer, A. M., Willis, M.W., Herscovitch, P., Daube-Witherspoon, M., Repella Shelton, J., Brenda, E. Benson, J.B., Post, R.M. & Wassermann, E. M. (2003a). Intensity-dependent regional cerebral blood flow during 1Hz repetitive Transcranial Magnetic Stimulation (rTMS) in healthy volunteers studied with H2 15O Positron Emission Tomography: I. effects of primary motor cortex rTMS. Biological Psychiatry, 54, 818–825. doi:10.1016/S0006-3223(03)00002-7

Speer, A. M., Willis, M.W., Herscovitch, P., Daube-Witherspoon, M., Repella Shelton, J., Brenda, E. Benson, J.B., Post, R.M. & Wassermann, E. M. (2003b). Intensity-dependent regional cerebral blood flow during 1Hz repetitive Transcranial Magnetic Stimulation (rTMS) in healthy volunteers studied with H2 15O Positron Emission Tomography: II. effects of prefrontal cortex rTMS. Biological Psychiatry, 54, 826–832. doi:10.1016/S0006-3223(03)00324-X

Spielberger, C. D. (1983). Manual for the State–Trait Anxiety Inventory (Form Y). Palo Alto, A: Mind Garden.

Taylor, P.C.J., Nobre, A. & Rushworth, M.F.S. (2007). Subsecond changes in top-down control exerted by human medial frontal cortex during conflict and action selection: a combined transcranial magnetic stimulation – electroencephalography study. The Journal of Neuroscience, 27(42), 11343–11353. doi:10.1523/JNEUROSCI.2877-07.2007

Thompson-Schill, S. L., Bedney, M., & Goldberg, R.F. (2005). The frontal lobes and the regulation of mental activity. Current Opinion in Neurobiology, 15, 219-224. PMID: 15831406. doi:10.1016/j.conb.2005.03.006

Van der Ploeg, H.M. (2000). Handleiding bij de Zelf Beoordelings Vragenlijst (ZBV). Swets & Zeitlinger, Lisse.

Van der Ploeg, H. M., Defares, P. B., & Spielberger, C.D. (1980). Handleiding bij de Zelf-Beoordelings Vragenlijst, ZBV. Een Nederlandstalige bewerking van de Spielberger State-Trait Anxiety Inventory, STAI-DY. Swets en Zeitlinger, Lisse.

Volman, I, Toni, I, Verhagen, L & Roelofs, K. (submitted). Endogenous testosterone modulates perfrontal-amygdala connectivity during social emotional behaviour.

Wang, Z., Aguirre, G.K., Rao, H., Wang, J., Fernández-Seara, M.A., Childress, A.R. & Detre, J.A. (2008). Emperical optimization of ASL data analysis using an ALS data processing toolbox: ASLtlbx. Magnetic Resonance Imaging, 26(2), 261-269. doi:10.1016/j.mri.2007.07.003

Audiovisual integration in head-unrestrained macaque monkeys

Marijn Bart Martens[1]
Supervisors: Rob van der Willigen[1], John van Opstal[1]

[1]*Donders Institute for Brain, Cognition and Behaviour, Radboud University, Nijmegen,*
The Netherlands

To rapidly orient gaze to relevant stimuli in the environment, the brain has to select the target from the background, determine its coordinates for the appropriate motor actions, and program the coordinated eye-head movement. Recently, we have extended the double-magnetic induction technique (DMI) for eye-movement recording to head-unrestrained conditions in humans. Here, we report on the application of our novel DMI technique to eye-head gaze shifts of trained macaque monkeys toward visual, auditory and combined audiovisual targets. Three macaque monkeys were surgically prepared for DMI recordings by implanting a thin golden ring behind the conjunctiva of the right eye and they were trained to make rapid gaze saccades to stimulus locations within the two-dimensional frontal hemifield. Head- (coil) and eye-(ring) movements were tracked independently in space through magnetic induction from three orthogonal oscillating magnetic fields. We used behavioural paradigms to study audiovisual integration and examine eye-head coordination during localization. We find that azimuth localization is comparable for all modalities, but elevation accuracy is degraded for auditory targets. Gaze onset times to visual and audiovisual targets are comparable, but faster than auditory localization. Interestingly, we find that the head onset is similar for all modalities, whereas the eye onset is delayed in auditory localization. We compared the gaze response times to the statistical facilitation predicted by the summation race model. The differences between observed and predicted responses provide evidence for neural integration during bimodal stimulus presentation.

Keywords: monkey, sound localization, audiovisual integration, Race model, Eye-head coordination.

1. Introduction

Many objects in the environment of humans and animals provide sensory information through multiple modalities. Imagine a game of soccer. Your teammate manages to lose his defender and now cues you to pass him the ball, providing a waving arm (visual cue) and shouting your name (auditory cue); allowing you to quickly and accurately locate your teammate and pass the ball. It has been shown that such multimodal information can lead to a reduction in response times (RTs) and an improvement in localization accuracy of saccadic eye movements (Corneil et al., 2002). The first report of an auditory facilitation effect showed that manual responses to a visual target decrease in RT (20-80 ms) when paired with an auditory stimulus (Todd, 1912).

The brain can apparently integrate signals from sensory modalities with completely different initial target representation: the visual world is encoded in a retino-centric way, whereas auditory cues are represented tonotopically and in a head-centered reference frame (Goossens & van Opstal, 1999). It is however not trivial how these different representational formats and different reference frames can be combined. To understand the neural basis subserving this integration, monkey recordings have focused on the role of parietal cortex (Avillac et al., 2007) and deep layers of the superior colliculus (Sparks, 1991; Frens & van Opstal, 1998). In these studies, gaze orienting is often used to train monkeys or study the localization behavior of visual and auditory localization. However, for technical reasons, the monkeys stay head-fixed.

Recently, Populin (2006) stressed the importance of a head-unrestrained model for sound localization. Monkeys showed better sound localization behavior towards auditory targets in the head-unrestrained condition when compared to the head-fixed condition.

To record gaze (eye-in-space), the most commonly used electromagnetic method is the scleral search coil technique (SSC) technique (Robinson, 1963). However, this method requires a lead wire to leave the eye to connect to the recording hardware. In experimental animals and patients the lead wires have proven to pose a considerable risk because they are prone to breakage. To avoid such vulnerable wires, it is possible to make use of double magnetic induction (DMI). The DMI method uses a gold-plated copper ring in which magnetically induced alternating currents generate small secondary magnetic fields that are determined by the ring's orientation. These signals are picked up by a coil, which is placed in front of the eyes (Bour et al., 1984); (Bos et al., 1988). Due to strong non-monotonic signal nonlinearities, the extreme sensitivity to mechanic vibrations and the complex head-orientation dependent dc-voltages on the DMI signal, this technique could initially only be used in the head-fixed condition. Recently, the DMI method was used to measure head-unrestrained gaze shifts in humans (Bremen et al., 2007a). The resolution of the DMI technique (0.3 deg) is comparable to the resolution of the SSC technique (0.2 deg). We extended the DMI method to record head-unrestrained gaze shifts in monkeys (Bremen et al., 2010).

Here we report on head-unrestrained macaque monkeys orienting to visual, auditory and audiovisual targets with high resolution stimulus presentation, and using the novel DMI technique to record head and gaze orientation. We examine audiovisual integration and test whether bimodal responses exceeded the responses predicted by statistical facilitation models, which would provide evidence for audiovisual neural interactions to response facilitation.

2. Methods

2.1 Subjects

Three adult monkey (Macaca mulatta: MA, OR, WO) were surgically prepared for DMI recordings by implanting a thin golden ring behind the conjunctiva of the right eye (Bour et al., 1984). A stainless-steel cap was attached to the skull on which the DMI recording setup could be mounted. Three monkeys were trained on the task and showed similar behaviour. One full dataset was recorded from monkey MA and is reported on here. All experiments were conducted in accordance with the guidelines for the use of laboratory animals provided by the Society for Neuroscience, and the European Communities Council Directive of November 24, 1986 (86/609/EEC). All experimental procedures were approved by the local ethics committee (DEC) for the use of laboratory animals at the Radboud University Nijmegen.

2.2 Experimental setup and stimulus presentation

Experiments were conducted in a completely dark, sound-attenuated room (2.5 x 2.5 x 2.5 m³),

of which the walls, ceiling, and floor were covered with black acoustic absorption foam that eliminates acoustic reflections down to 500 Hz (Schulpen Schuim, Nijmegen, The Netherlands). Subjects were comfortably seated in a primate chair designed to permit unrestricted movements of the head. Target stimuli were always presented sequentially.

Auditory stimuli (A) were presented through broad-range speakers (Visaton GmbH SC5.9) with a flat frequency characteristic within 5 dB between 0.2 and 20 kHz after equalization. On a rotating arch, 32 speakers were mounted with 5° spacing in elevation (range: -70° to +85°) and an azimuth resolution of <0.1° (range: 360°). Auditory localization cues were Gaussian white noise with on- and offset ramps of 0.5 ms). Acoustic stimuli were digitally generated using a RX6 Tucker-Davis System at 50-kHz sampling rate (Tucker-Davis Technologies, Alachua, FL) and send to one of the speakers in the experimental room. The sound on- and offset was triggered by a micro-controller with millisecond precision and implemented using the RPvds graphical language.

Visual stimuli (V) could be presented through green light-emitting diodes (LEDs) mounted on a acoustically transparent wire frame that contained twelve spokes (arranged at 30° intervals) at radii of 5, 9, 14, 20, 27, 35 and 44 degrees, resulting in 85 additional possible locations. In the reference position, the head of the subject was aligned with the central LED (0, 0°) at a distance of 1.2 m. LED intensities were calibrated to provide equal intensity for all visual stimuli. Every speaker on the arch also contained a green LED to present visual stimuli (radial distance 1.0 m with 5° spacing in elevation (range: -70 to +85°) and azimuth resolution of <0.1° (range: 360°).

2.3 Recording of eye and head orienting

The two-dimensional orientation of the eye was measured using the DMI method. Calibration data were collected using an intensity change detection task. The intensity difference was subtle (20%), such that foveating the LED was necessary for detection. Magnetic induction from three orthogonal oscillating magnetic fields in the pick-up coil of the DMI setup was recorded at 1017.25 Hz per channel (RA16, Tucker-Davis Technologies, Alachua, FL). The magnetic fields were driven by custom-built amplifiers (horizontal, vertical and frontal, at 48, 60, 80 kHz respectively). The effective components for the three magnetic fields were detected using PAR lock-in amplifiers (Princeton Applied Research 128A) and were low-pass filtered using a custom

filter (4th order Butterworth, 150 Hz). Response data were stored offline and calibrated by training two three-layered neural networks (6 hidden units), one for the azimuth component and the other for the elevation component. Head orientation was measured using the search coil technique. To collect head calibration data, a laser pointer was attached to the head stage. The experimenter manually oriented the head to LEDs at known positions and response data was also calibrated using two three layered neural networks. A calibration session was typically between 100 to 200 trials. After calibration, gaze and head orientation were visualized online.

2.4 Experimental task

The task for the subject was to rapidly foveate the location of auditory, visual or audiovisual targets. To start a trial, the monkey had to release a handle bar while the red fixation light was on. A green fixation light appeared (always centered at 0,0°). Maintaining gaze for 150 ms (within the first second after releasing the bar) in a computer defined acceptance window (10° in elevation and azimuth) initiated a sequence of targets in the periphery. In this sequence, 1 to 5 visual targets at random locations appeared and had to be foveated quickly. If the monkey maintained gaze within the acceptance window for 300 ms, the trial would advance to the next target. The final target could be an auditory, visual or audiovisual target. The auditory and visual onset times could be manipulated. Gaze had to be in the acceptance window of the final target within 400 ms and maintained for another 300 ms before acquiring the reward.

2.5 Behavioral training and reward

To train the monkey to make saccades to broadband auditory targets, we first presented aligned audiovisual targets. After the monkey got accustomed to the presence of the sound stimulus, we decreased the stimulus strength of the visual target, and occasionally only present an auditory stimulus. During these initial auditory only trials, the acceptance window was increased (20° azimuth and elevation) to avoid frustration. The percentage of broadband auditory targets increased and the acceptance window could be slightly reduced (10° azimuth and 16° elevation). After the monkey learned to make saccades to auditory targets, no further effort was made to decrease the size of the acceptance window. The monkeys were unable to

localize sounds in the bottom half of the hemifield, possibly because of acoustic blocking or interfering of the primate chair. We therefore only presented stimuli from -10° to +60° elevation. For water reward delivery a thin stainless steel tube was mounted on the DMI assembly which was connected to a water reservoir outside the experimental chamber by a silicone rubber tube.

2.6 Dependent variables and data analysis

Gaze position at the end of the first saccade after target presentation was the measure of localization behaviour. Target and response coordinates are expressed in the azimuth and elevation coordinates of the double-pole coordinate system (Knudsen & Konishi, 1979). The target was presented until the end of the trial. Because the monkey was performing a multistep target localization experiment with short inter-target-intervals, we used stringent velocity criterions: saccade response time (SRT) when gaze velocity surpassed 200 deg/s and head response time (HRT) when the head motion exceeded 25 deg/s. The saccade was required to start within the first 400 ms of the trial. Eye signals were simply calculated by subtracting the head from the gaze signal. Localization error was the absolute difference between the target location and the gaze position at the end of the first localization saccade, before any correction saccades. Initial localizations that were outside a tolerance window of 30 deg (azimuth and elevation) were removed, but appeared to be sparse. Errors were plotted using ellipses of 1 SD width centered at the mean. For saccade accuracy, the optimal linear fit of the stimulus-response relation between saccade amplitude and target eccentricity was found by minimizing the sum-squared deviation of

$$\alpha R = a + b \cdot \alpha T \quad \text{and} \quad \varepsilon R = c + d \cdot \varepsilon T \tag{1}$$

for the azimuth (α) and elevation (ε) components, respectively. In equation 1, a and c are the response biases in degrees (offset of the fitted line), and b and d are the response gains (slopes). To determine the gaze and head traces, the recorded voltage position signals were first lowpass filtered (cut-off frequency 75 Hz, filter order 50). Data analysis and visualization was performed using custom-written Matlab (The MathWorks, Natick, MA) programs.

2.7 Race Model

The race model postulates that the reaction time to a bimodal stimulus is simply the reaction to whichever stimulus was perceived first (Raab, 1962). This race model thus accounts increased reaction time to statistical facilitation: the time to detect one of two stimuli is faster than the time to detect a single stimulus. Special distributional assumptions included in the race model have been developed, such as stochastic independence between channels (Gielen et al., 1983) or Bayesian integration (Battaglia et al., 2003). We will test whether the observed responses are faster than statistically predicted by the classical race model of probability summation (eq. 2).
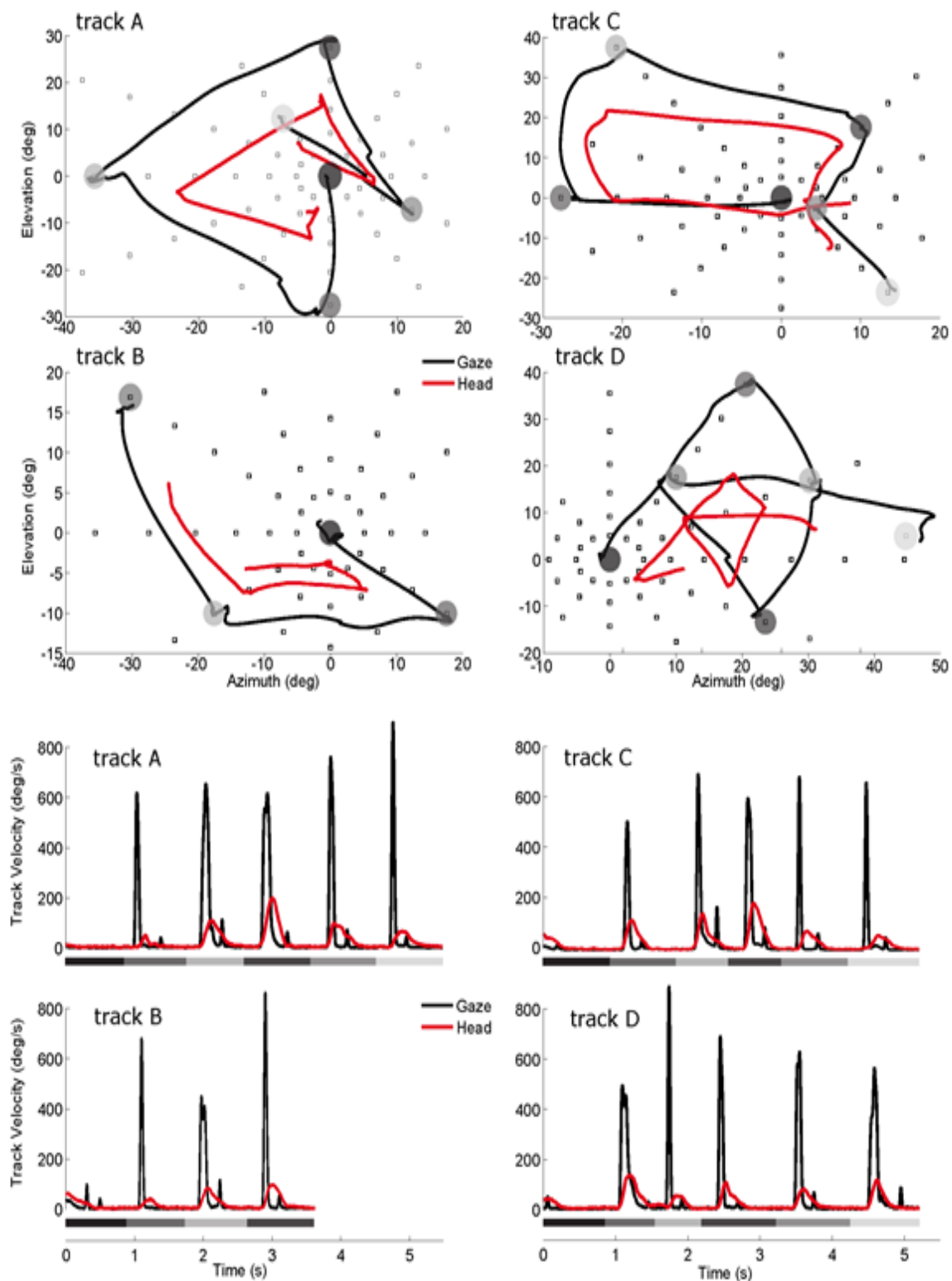
$$R(\tau) = A(\tau) + V(\tau) \tag{2}$$

Where τ is a given SRT, $A(\tau)$ and $V(\tau)$ are the cumulative probability distributions for that particular SRT. If the observed SRTs are faster than predicted by the race model, the signals from both modalities are neutrally integrated prior to saccade initiation (Hughes et al., 1994; Nozawa et al., 1994). Because the summation race model has stringent constraints on statistical facilitation, predicting neural integration is conservative. Also, slower reaction times than predicted by the race model indicate neural integration (i.e. one of the stimuli is partially ignored). However, the summation race model is liberal for detecting slower responses. To determine the mean deviation between the observed and predicted data, (model – observed), the cumulative probability distribution was averaged (excluding extremities, 10% and 90% cut-off).
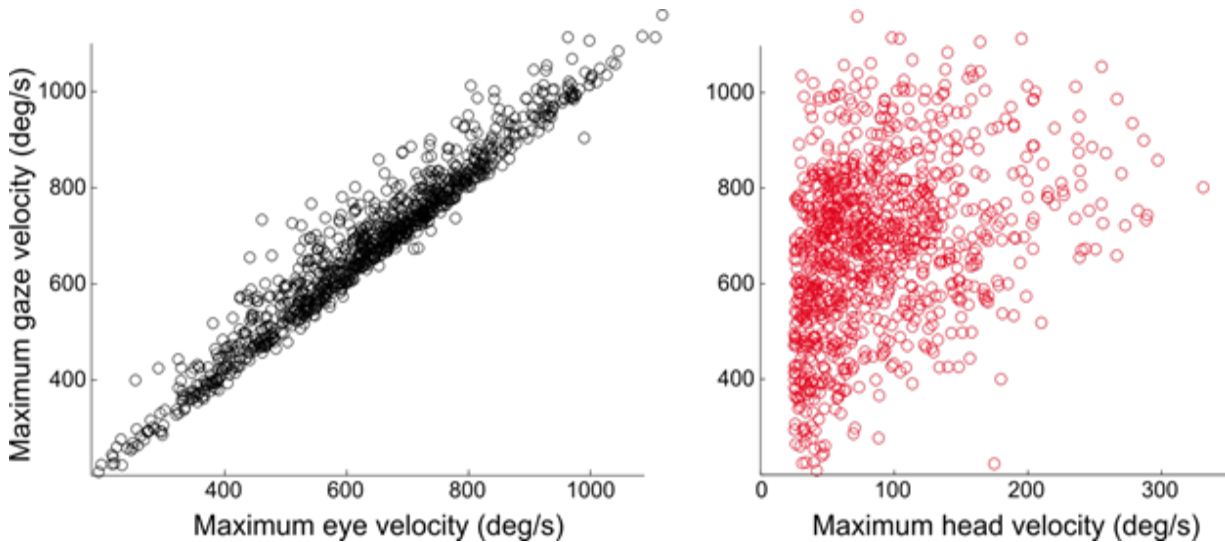
3. Results

3.1 Calibrated gaze and head profiles

We report on gaze and head profiles of experimental animals recorded with the DMI technique (Figure 1). Four track profiles of the visual-jump paradigm (sequential targets at different locations) are shown (top half), where the monkey sequentially tracked up to 6 visual targets. The vectorial velocity profiles belonging to these four tracks (bottom half) show saccadic responses with velocities exceeding 800 deg/sec and head movements of up to 200 deg/sec. Typically, the head does not reach the target locations and lags slightly behind the saccade onset (Goossens & Opstal, 1997). Thus, when the monkey's gaze has

Fig. 1 Examples of calibrated gaze (black line) and head (red line) trajectories of monkey MA for four different trials (A-D) of the visual-jump paradigm. The monkey was rewarded when correctly reporting dimming of the last visual target (light grey) by releasing a handle bar. Because the number of targets cannot be anticipated, the monkey has foveated all intervening targets (darker gray circles) as well. The darkest gray circle indicates the initial fixation point at (0,0) deg. Note that eye-in-space and head-in-space follow very similar, but not identical, trajectories. The lower half of the figure shows the associated vectorial velocity profiles of gaze and head as a function of time, as well as the stimulus presentation times. The track velocities show a clear peak for the saccade, often followed by a correction saccade, characterized by a small bump. After these initial saccades, the track velocity is near zero; the monkey is stably fixating the target. Despite substantial head movements, the peak head velocities (∼ 200 deg/s) are much lower than the gaze velocities (up to 900 deg/s).

Fig. 2 Eye and head maximum velocity compared to the maximum gaze shift. Note that the increase in maximum head velocity is nonlinear; the relative maximum head velocity decreases for larger gaze velocities.

already reached the target location, the head is still in motion. The vestibulo-ocular reflex counterrotates the eye while the head is still moving. This allows the recording of multiple eye-head orientations while the subject is fixating, allowing us to reduce the total number of trials needed for calibration.

We examined the contributions of the eye and head to saccadic localization. Figure 2 shows the nonlinear behaviour of head peak velocity compared to the gaze peak velocity: as the peak velocity of the gaze increases, the relative head peak velocity decreases. We normalized the azimuth and elevation component of the gaze trajectory and used the same normalization factors for the head trajectories. The normalized head paths and endpoints, which deviate to direction of total gaze movement (Figure 3).

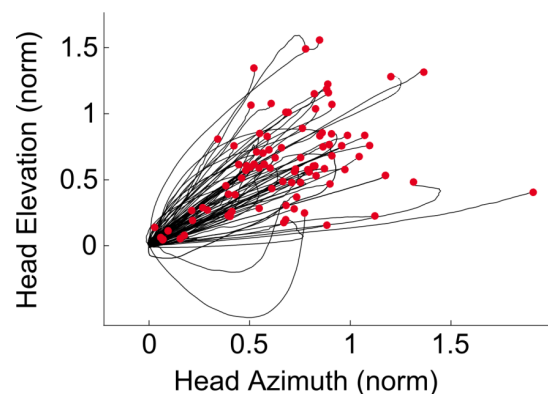## 3.2 Audiovisual localization accuracy

Figure 4 and Figure 5 show the localization accuracy and localization error as a function of SRT. Described here is the accuracy of the initially saccade, excluding any correction saccades. Azimuth localization to targets of all modality types was comparable. However, broadband auditory elevation errors were large, with an upward bias and lower gain.

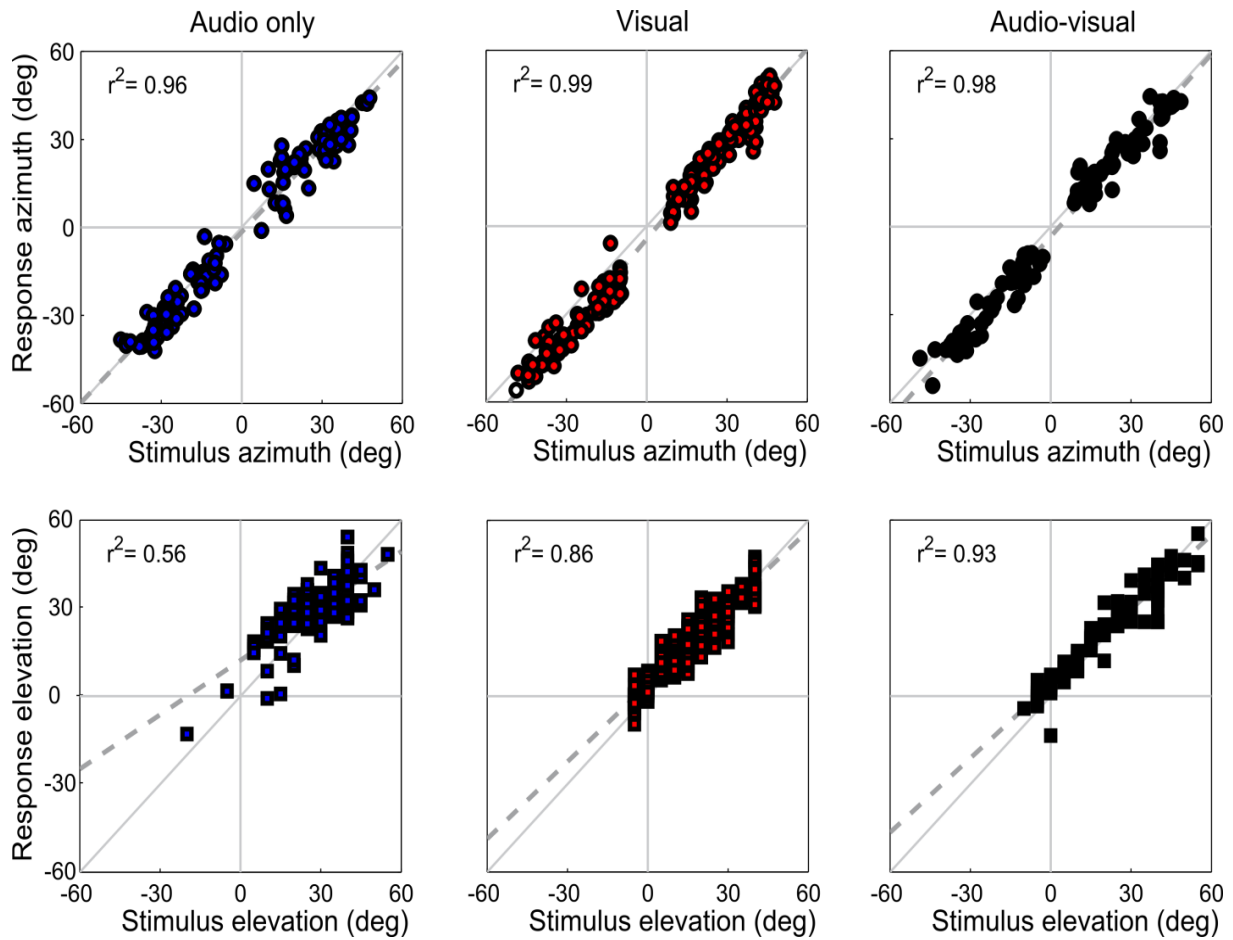## 3.3 Audiovisual integration: observed and predicted SRTs

SRTs to auditory (A) targets were longer compared to visual (V) targets (Figure 6). Responding to temporally synchronous AV stimuli yielded faster

SRTs compared to unimodal A stimuli, but not compared to V trials. When the monkey responded to temporally asynchronous bimodal stimuli, the SRTs increased. When an A stimulus appeared first (i.e. A50V), the SRTs increased. This trend was continued for longer lags of V stimulus onset. Also, when the V stimulus appeared first (i.e. V50A), the SRTs increased. The auditory stimulus thus delayed the SRT, summarized by the trend (red line) for temporally unsynchronized AV stimuli.
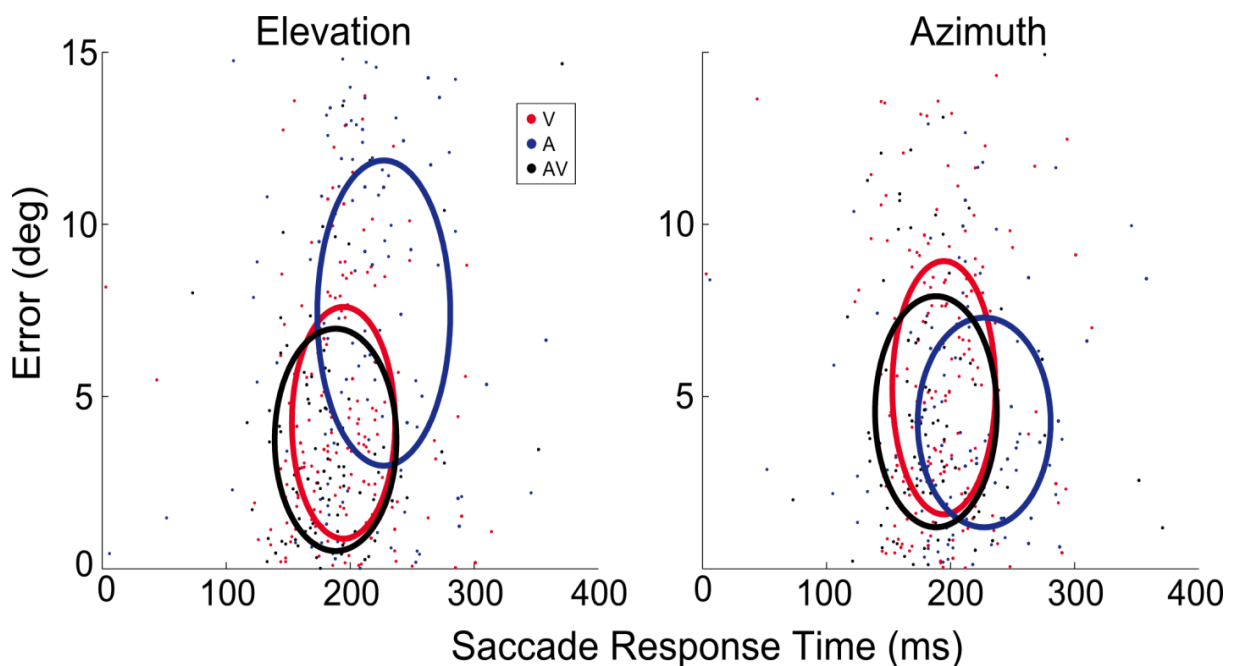
When we examine the overall gaze SRT and HRT distributions, the head appears to lead the gaze (Figure 7, left side). It is however difficult to determine the exact onset times. Studying the relative deviation between gaze and head for the modalities (right side), shows in a trial-by-trial analysis that for A targets compared to V or AV targets, the gaze is slower (~50 ms) than the head (p<0.001).

Fig. 3 The normalized head contribution to saccadic gaze shifts. Each azimuth and elevation head component is normalized to gaze endpoint (1,1). The deviation from the unity line shows that the head and eye behave differently.

Fig. 4 Accuracy of AV gaze shifts outperforms unimodal (A or V) responses. Note that the monkey generates accurate auditory evoked gaze shifts when the head is unrestrained. Although A azimuth localization is comparable to V or AV, elevation has an upward bias and lower gain.
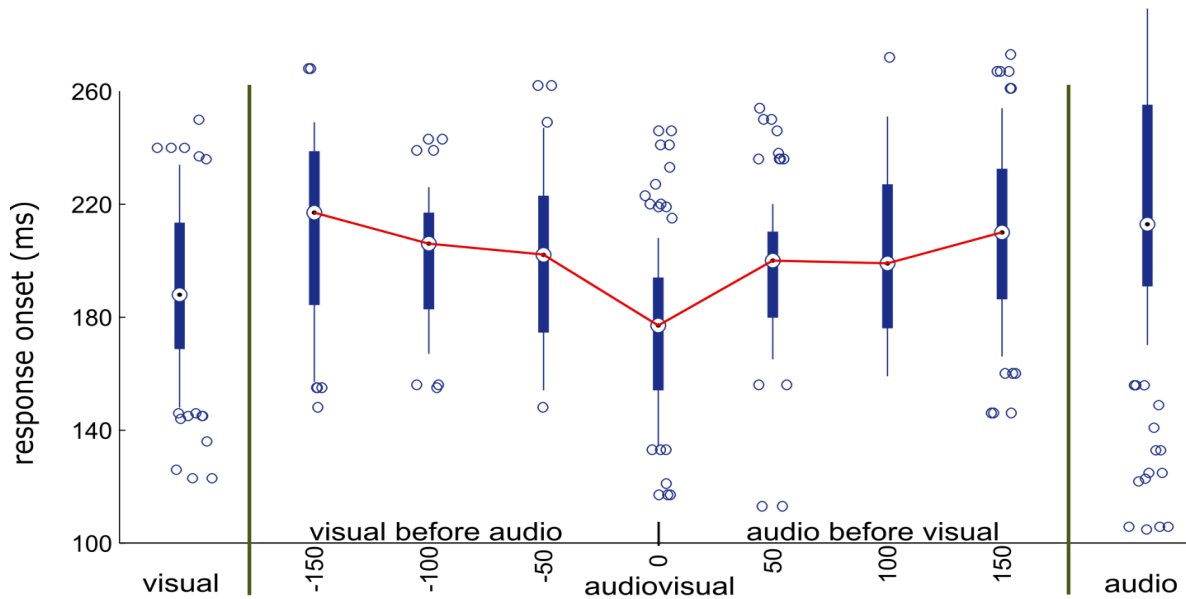

Fig. 5 Localization errors as a function of SRT. Although azimuth errors are similar for all modality types, A elevation errors exceed V or AV localization errors.
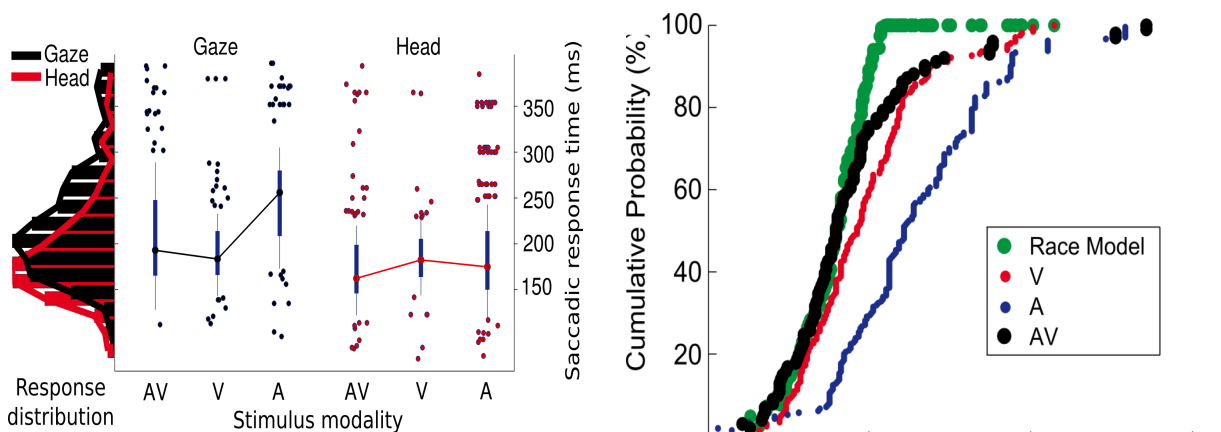
The observed cumulative probability distributions for A, V and AV targets as well as the distribution predicted by the summation race model are shown in Figure 8. The AV distribution is prior to A and slight prior to V distribution SRTs and is guided by the summation race model trend without exceeding it (until cumulative distribution reaches ~80%).

Figure 9 shows the observed and predicted cumulative probability distributions for temporally asynchronous stimuli. The response distribution of th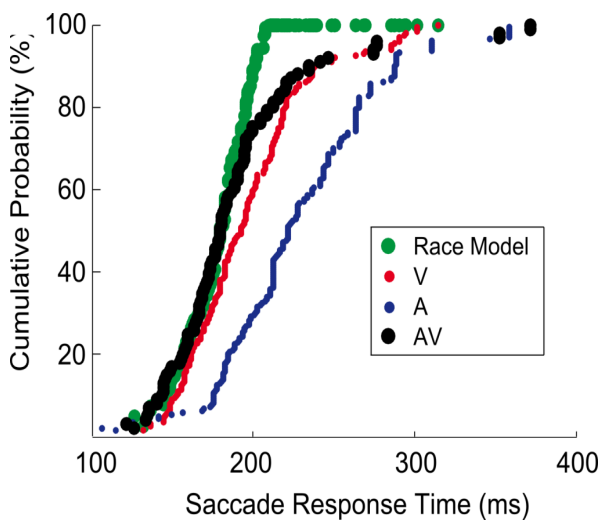e lagging stimulus is simply a shifted (by the delay time) version of the unimodal stimulus distribution. This shifted distribution is used to calculate the summation race model. For the SOAs we can observe clear differences between the observed and predicted SRTs. For A targets proceeding V, SRTs are shorter than predicted by the race model. On trials with the auditory stimulus lagging 150 ms, the SRTs are delayed compared to unimodal V trials as well as predicted by the race model. The mean deviation summarizes the difference between observed and predicted SRTs (Figure 10).

Fig. 6 SRTs for unimodal and bimodal stimuli with temporal synchronous and asynchronous presentation. Responses to A are slower than V (P < 0.001) as well as to both AV (P < 0.001). The trend shows that a V target, either temporally aligned or presented shortly after an A target, facilitates reaction time. V responses were not statistically slower than aligned AV (P = 0.14). However, both V stimuli prior or followed by an A stimulus were slower than aligned AV (see red trendline).

Fig. 7 Gaze SRT and HRT distributions (left) for the different stimulus modalities (right). HRT appear to lead the gaze SRT, but determining the exact onset times is difficult. However, the relative difference between gaze and head for the modalities show in a trial-by-trial analysis that for A targets compared to V or AV targets, the gaze is slower (~50 ms) than the head (p < 0.001).

Fig. 8 Cumulative probability distribution for the observed SRTs for visual (red), auditory (blue) and temporally aligned audiovisual (black) targets. The predicted SRTs of the race model (green) depend on the distributions of the visual and auditory responses.

Fig. 9 Cumulative probability distributions for the observed SRTs and race model for the SOAs. The observed SRTs shift compared to the race model for the different SO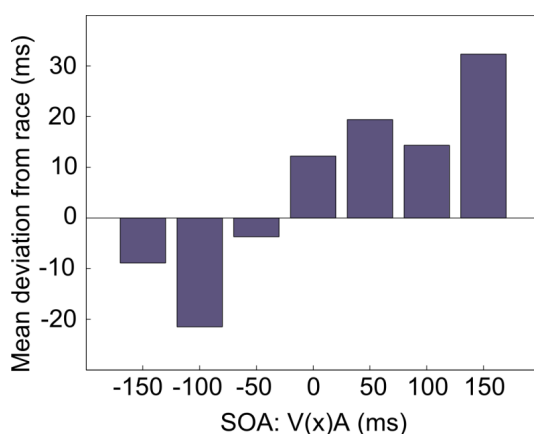As. For targets with A proceeding V, SRTs are shorter than predicted by the race model. These faster responses can therefore not be explained by statistical facilitation and indicate neural integration. On trials with the auditory stimulus lagging 150 ms behind V, the SRTs are delayed compared to broadband V trials as well as predicted by the race model.

Fig. 10 Summary of SRT responses (observed) to the race model (predicted) across SOAs. For trials where the visual stimulus lags on the auditory stimulus (i.e. V-150A), the observed responses are faster than predicted by the race model. When the auditory stimulus lags on the visual stimulus (i.e. V150A), the observed responses are slower than predicted by the race model. This clear trend demonstrates that statistical facilitation does not accurately explain the increase in observed responses, opting for neural integration prior to saccadic initiation.

4. Discussion and conclusions

4.1 DMI method for recording monkey gaze orientation.

We successfully applied the DMI method for recording head unrestrained monkey gaze orientation during visual, audio and audiovisual target localization. The importance of a head unrestrained monkey for sound localization was already established. We used this technique in demonstrating gaze tracking with audiovisual integration to spatially aligned bimodal targets.

4.2 Gaze and head profiles

We observed the nonlinear behaviour of head velocity compared to the peak gaze velocity (Freedman & Sparks, 1997). As the gaze velocity increases, the total head contribution relatively decreased. Also, the azimuth and elevation direction components of the head normalized to the total gaze showed that the head movement differs from the eye movement direction. These differences in motor execution can be due to either different control systems for eye and head (Freedman, 2008) or simply due to different kinematics. If the head, eye and their azimuth and elevation components are controlled by separate independent systems, these complex trajectories could be planned, possibly for specific strategies such as minimum variance (Harris & Wolpert, 1998; Tanaka & Qian, 2006), minimum torque (Uno & Suzuki, 1989; Tanaka & Qian, 2004) or another optimal motor control plan. However, the observed trajectories of the eye and head could also be due to the kinematics properties of the two systems. The systems could share an input signal and under appropriate feedback control the target will be reached. Simple muscle properties could be the cause for such observed behaviour. In our experiments, we are unable to distinguish what causes the nonlinearity in the observed trajectories.

4.3 Audiovisual localization accuracy

We demonstrated monkey localization to a wide range of targets in the frontal hemifield using auditory, visual and combined audiovisual stimuli. Azimuth localization to targets of all modality types was comparable, with a gain near 1 and low localization errors. Elevation errors to auditory targets however were large, with an upward bias and lower gain. The larger localization errors to auditory

targets as well as a lower gain are also typically observed in humans (Corneil et al., 2002), but could be due to acoustic interfering of the primate chair.

4.4 Audiovisual integration: observed and predicted SRTs

Responding to temporally synchronous audiovisual stimuli yielded faster SRTs than unimodal auditory stimuli, but not compared to visual trials. In humans, shortened reaction times to auditory stimuli are often reported, but may depend on relative stimulus intensity (Bell et al., 2001). When temporally asynchronous bimodal stimuli were presented, the SRTs increased for both auditory targets leading as well as when visual targets were presented first. Such bidirectional increase already indicates interaction between the two modalities.

When we examine the overall gaze SRT and HRT distributions, the head appears to lead the gaze. However, because the monkeys perform a multistep localization task with short inter-target-intervals, we used stringent criteria for head and gaze onset. The head and eye have different acceleration profiles, such that determining the absolute onset of the eye and head is ambiguous and difficult to compare. However, comparing the relative difference in onset between the auditory, visual and audiovisual conditions revealed that the gaze onset is delayed to the head onset in auditory compared to visual and audiovisual localization. The head moving relative early compared to the eye in auditory trials possibly relates to auditory tonotopical representation and a head-centered reference frame (Goossens & van Opstal, 1999).

We compared the observed SRTs with the statistical facilitation predictions described by the summation race model. For bimodal targets with the auditory stimulus lagging on the visual stimulus, responses are slower than predicted. The interference observed here suggests neural integration of the modalities instead of separate processing. More clearly however, with the auditory stimulus leading the visual stimulus, the responses are faster than predicted. These differences in observed and predicted SRTs argue that bimodal stimuli provide more information than can be explained by statistical facilitation and provide evidence for neural integration of the two modalities during localization behaviour.

References

Avillac, M., Ben Hamed, S. & Duhamel, J., 2007. Multisensory Integration in the Ventral Intraparietal Area of the Macaque Monkey. J. Neurosci., 27(8), 1922-1932.

Battaglia, P.W., Jacobs, R.A. & Aslin, R.N., 2003. Bayesian integration of visual and auditory signals for spatial localization. Journal of the Optical Society of America. A, Optics, Image Science, and Vision, 20(7), 1391-1397.

Bell, A.H., Corneil, B.D., Meredith, M.A. & Munoz, D.P., 2001. The influence of stimulus properties on multisensory processing in the awake primate superior colliculus. Canadian Journal of Experimental Psychology = Revue Canadienne De Psychologie Expérimentale, 55(2), 123-132.

Bos, J.E., Reulen, J.P., Boersma, H.M. & Ditters B.J., 1988. Theory of double magnetic induction (DMI) for measuring eye movements: correction for nonlinearity and simple calibration in two dimensions. Biomedical Engineering, IEEE Transactions on, 35(9), 733-739.

Bour, L. J., van Gisbergen, J. A. M., Bruijns, J. & Ottes, F. P., 1984. The Double Magnetic Induction Method for Measuring Eye Movement - Results in Monkey and Man. IEEE Transactions on Biomedical Engineering, BME-31(5), 419-427.

Bremen, P., Van der Willigen, R.F. & Van Opstal, A.J., 2007a. Applying Double Magnetic Induction to Measure Two-Dimensional Head-Unrestrained Gaze Shifts in Human Subjects. J Neurophysiol, 98(6), 3759-3769.

Bremen, P., Van der Willigen, R.F. & Van Opstal, A.J., 2007b. Using double-magnetic induction to measure head-unrestrained gaze shifts. I. Theory and validation. Journal of Neuroscience Methods, 160(1), 75-84.

Bremen, P., Van der Willigen, R.F, Van Wanrooij, M.M., Schaling, D.F., Martens, M.B., Van Grootel T.J., & Van Opstal, A.J., 2010. Applying double-magnetic induction to measure head-unrestrained gaze shifts: calibration and validation in the monkey. Biological Cybernetics, DOI 10.1007/s00422-010-0408-4.

Corneil, B.D., van Wanrooij, M., Munoz, D.P. & van Opstal, A.J., 2002. Auditory-Visual Interactions Subserving Goal-Directed Saccades in a Complex Scene. J Neurophysiol, 88(1), 438-454.

Freedman, E.G., 2008. Coupling between horizontal and vertical components of saccadic eye movements during constant amplitude and direction gaze shifts in the rhesus monkey. Journal of Neurophysiology, 100(6), 3375-3393.

Freedman, E.G. & Sparks, D.L., 1997. Eye-Head Coordination During Head-Unrestrained Gaze Shifts in Rhesus Monkeys. J Neurophysiol, 77(5), 2328-2348.

Frens, M.A. & Van Opstal, A., 1998. Visual-auditory interactions modulate saccade-related activity in monkey superior colliculus. Brain Research Bulletin, 46(3), 211-224.

Gielen, S.C., Schmidt, R.A. & Van den Heuvel, P.J., 1983. On the nature of intersensory facilitation of reaction time. Perception & Psychophysics, 34(2), 161-168.

Goossens, H.H.L.M. & Opstal, A.J.V., 1997. Human eye-head coordination in two dimensions under different sensorimotor conditions. Experimental Brain Research, 114(3), 542-560.

Goossens, H. & van Opstal, A., 1999. Influence of Head Position on the Spatial Representation of Acoustic Targets. J Neurophysiol, 81(6), 2720-2736.

Harris C.M. & Wolpert D.M. 1998. Signal-dependent noise determines motor planning. Nature, 394:780-784.

Hughes, H.C., Reuter-Lorenz, P.A., Nozawa, G. & Fendrich, R., 1994. Visual-auditory interactions in sensorimotor processing: saccades versus manual responses. Journal of Experimental Psychology. Human Perception and Performance, 20(1), 131-153.

Knudsen, E. I. & Konishi, M., 1979. Mechanism of sound localization in the barn owl. J. Comp. Physiol. A 133, 13–21.

Kawato M., Maeda Y., Uno Y. & Suzuki R. 1990. Trajectory formation of arm movement by cascade neural network model based on minimum torque-cahnge criterion. Biological Cybernetics, 62:275-288.

Nozawa, G., Reuter-Lorenz, P.A. & Hughes, H.C., 1994. Parallel and serial processes in the human oculomotor system: bimodal integration and express saccades. Biological Cybernetics, 72(1), 19-34.

Populin, L.C., 2006. Monkey Sound Localization: Head-Restrained versus Head-Unrestrained Orienting. J. Neurosci., 26(38), 9820-9832.

Raab, D.H., 1962. Statistical facilitation of simple reaction times. Transactions of the New York Academy of Sciences, 24, 574-590.

Robinson, D.A., 1963. A method of measuring eye movement using a scleral search coil in a magnetic field. IEEE Transactions on Bio-Medical Engineering, 10, 137-145.

Sparks, D.L., 1991. Sensori-motor integration in the primate superior colliculus. Seminars in Neuroscience, 3(1), 39-50.

Tanaka H., Tai M. Qian N., 2004. Different predictions by the minimum variance and minimum torque-change models on the skewness of movement velocity profiles. Neural Comput. 16(10):2021-40.

Tanaka H., Krakauer J.W. & Qian N., 2006. An optimization principle for determining movement duration. J. Neurophysiol. 95(6):3875-86.

Todd, J.W., 1912. Reaction to multiple stimuli, The Science Press.

Posture influences estimates of body representations during motor planning: an fMRI study

Marius Zimmermann[1]
Supervisors: Ruud GJ Meulenbroek[2], Floris P de Lange[1]

[1]*Donders Centre for Cognitive Neuroimaging, Nijmegen, The Netherlands*
[2]*Donders Centre for Cognition, Nijmegen, The Netherlands*

It is still an open issue how we generate motor plans to attain our goals. Several studies suggest that motor planning is a hierarchical process that is organized around the action outcome or goal. Moreover, action selection depends on the current state of one's own body. In this study we investigated how one's own body posture interacts with planning of goal-directed actions. Participants engaged in an action planning task while we manipulated their arm posture. Behavioral results indicate that motor planning is facilitated when one's own body state is congruent with the goal posture, rather than begin posture, of the planned movement. fMRI results showed that two regions that are involved in body representation, the intraparietal sulcus (IPS) and the extrastriate body area (EBA), showed an interaction between body posture and action planning. There was more activity in IPS when the body posture was overall incongruent with the action plan, whereas EBA was specifically more active when the body posture was incongruent with the goal posture of the planned action. This suggests that IPS maintains an internal state of both one's own body posture and the body posture used in a planned action, while EBA contains a representation of the action's goal posture. Together, our results indicate that movement planning is facilitated (in terms of behavioral performance and neural computation) by adopting the goal posture of the movement, in line with models that hypothesize that movement planning is organized around the specification of goal postures.

Corresponding author: Marius Zimmermann, Donders Institute for Brain, Cognition and Behavior, Radboud University Nijmegen, NL- 6500HB, Netherlands, Phone: +31 24 36 14731, Fax: +31 24 36 10652, E-mail: m.zimmermann@donders.ru.nl

1. Introduction

When we have a goal (such as drinking a cup of tea), the central nervous system (CNS) has to find a solution to achieve this goal, using a set of motor commands (e.g. reaching for and grasping of a cup, then moving it to the mouth). However, our body has abundant degrees of freedom (Bernstein, 1967), which enables us to achieve goals using a wide range of actions, but at the same time poses the problem that there is no unique solution. Selecting the optimal solution is a fundamental decision process that depends on both the state of our body and the context at hand (Kording and Wolpert, 2006).

It is generally assumed that the CNS selects actions that are optimal in respect to criteria like smoothness (Flash and Hogan, 1985) or energy costs (Alexander, 1997) of the movement. Crucially, motor planning appears to be organized around distal goals (Grafton and Hamilton, 2007). In line, Rosenbaum and colleagues suggest that, often, rather than optimized movement trajectories, optimized goal-states have highest priority in planning of goal-directed actions. Depending on the action's goal different criteria are optimized, for example precision in dancing or impact in boxing. Often it seems to be the comfort of end-postures that is maximized, at the cost of comfort of intermediate postures, which is known as the end-state comfort effect (Rosenbaum et al., 1992; 1995; 2001; 2009). For example, when a waiter wants to fill a glass that stands upside down on a table, he grasps the glass in an awkward way (thumb down) to turn it around, so he can hold it in a comfortable way (thumb up) during filling. But the suggestion that end-state comfort is optimized has been doubted by Herbort and Butz (2010), who suggest that, rather than optimizing the orientation of the goal state of an action, we make use of heuristic grip orientations when grasping objects for rotations (e.g. use a supine grip for counter clockwise rotations, and a prone grip for clockwise rotations).

Neurally, support for motor planning in terms of goal states is provided by Graziano et al. (2002). They applied microstimulation at behaviorally relevant timescales to neurons in premotor cortex of monkeys, which resulted in movements towards neuron specific postures, independent of the initial body posture. These neurons therefore represent goal states of the body rather than specific movements or muscles.

Behaviorally it has been shown that the ease with which motor plans are generated is affected by changing one's body posture (Sirigu and Duhamel,

2001). Therefore, planning may be facilitated when one's body state is congruent with an action's goal state. The CNS estimates body states using forward models (Grush, 2004) that are maintained in the intraparietal sulcus (IPS) of the parietal cortex (Wolpert et al., 1998; Wolpert and Ghahramani, 2000). Additionally, the extrastriate body area (EBA, Downing et al., 2001) seems to be involved in representing end-states of manual actions during motor preparation (Astafiev et al., 2004; Kuhn et al., in press). Previous research (de Lange et al., 2006) already reported modulation of activity in IPS by body posture during motor simulation, and EBA activation seems to be modulated by the availability of proprioceptive information in Parkinson's disease patients (Helmich et al., 2007).

Here, we want to investigate how one's own body posture interacts with motor planning. For this, participants engaged in a planning task involving grasping and placing of an object, while we manipulated their arm posture. In neural terms, we expect modulation of activity in IPS and EBA by body posture in motor planning. Behaviorally, we expect planning to be facilitated when one's body posture is congruent with the goal-posture of the planned movement, in case start- and goal-posture of the planned action differ from each other, such as when the waiter turns the glass right-side up. This would support the notion that action planning is organized around goals and, at a lower level, in terms of goal states of the body. On the other hand, facilitation by congruence between one's physical hand posture and an action's start posture could be expected from a heuristic approach to action selection, where the goal state is less important to plan an action.

2. Methods

2.1 Participants

Twenty participants (13 female) with an average age of 23.1±1.6 (mean±SD) years participated after giving informed consent according to institutional guidelines (CMO region Arnhem-Nijmegen, The Netherlands) for payment of 10 euros/hour or course credit. All of them were right handed and had normal or corrected-to-normal vision. One of the participants was excluded from the analysis of behavioral data because responses were not correctly recorded. Two others were excluded because of ideosyncratic performance on both motor execution and planning tasks (grip preference >3 SD from

mean grip preference).

2.2 Task

Participants engaged in a motor execution (ME) and motor planning (MP) task subsequently. We acquired functional magnetic resonance imaging (fMRI) data during the MP task only.

2.2.1 Motor execution (ME) task

Three cradles were positioned on a table next to each other at 5 cm distance between adjacent cradles. We instructed participants to grasp a bar (length: 25cm, diameter: 2.5cm) that was lying on the middle cradle using a full hand (power) grip and place it according to instructions we presented on a screen. One half end of the bar was painted black, the other half white. Instructed actions always involved a direction (i.e. whether to place the bar on the left or right cradle), and final bar-orientation (Figure 1).
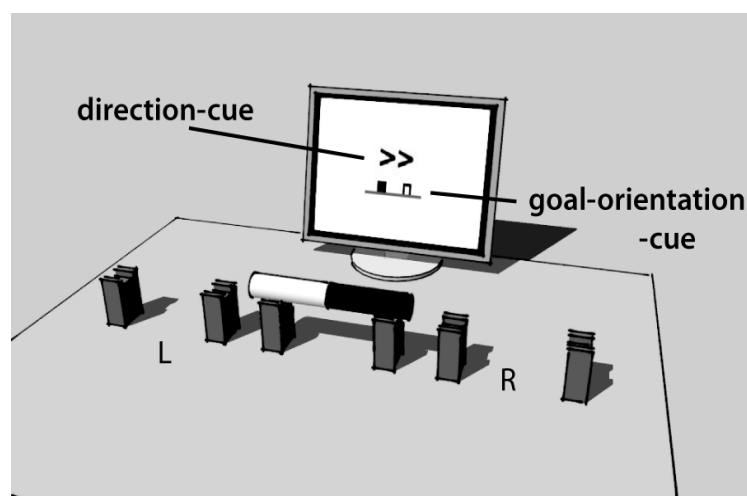
Some actions required a simple translation of the bar from the middle cradle to the left or right cradle, whereas other actions required a 180 degrees rotation. We also included trials in which the bar had to be placed vertically (requiring a 90 degrees rotation), to allow for comparison with earlier studies (Rosenbaum et al., 1992). Each trial started with the bar lying on the middle cradle, with the white end either to the left or right side. We instructed participants to rest their hand on the table prior to every trial with the palm facing either up or down, changing after every eighth trial. During the task, we tracked participants' hand position using a three-dimensional motion tracking device (Polhemus Liberty, using 2 sensors at the left and right edge of

the wrist of the right arm, sampling at 240 Hz). We established movement times and grip choice from these recordings offline.

2.2.2 Motor planning (MP) task

Participants engaged in a motor planning task while whole-brain activity recordings were made using fMRI. During the MP task, participants saw a picture of a bar on the middle one of three cradles, representing the start configuration of trials in the ME task. We used the same instructions to signal the desired goal orientation and position of the bar (Figure 2), but in the MP task we asked our participants to report "where they would place their thumb on the bar" in order to move the bar from starting to goal position. They indicated whether they would place their thumb on the black or white end of the bar, using one of two buttons with their index and middle finger of their left hand. We established reaction times and grip choice from these responses.

During the MP task, we manipulated participants' right arm posture: participants had to keep their right hand in a palm up or palm down orientation for blocks of eight trials. Since no overt movements had to be performed, hand posture did not change during a trial. This resulted in different patterns of congruency between a subject's own hand posture and the hand posture(s) during planned hand movements. During trials requiring no bar rotation but only bar translation (NO ROTATION trials), participants' posture could either be 'overall congruent' or 'overall incongruent' with the planned action (because the start- and goal-posture are the same for these actions, see Figure 2). During trials requiring a bar rotation (ROTATION trials),

Fig.1 Motor execution (ME) task. A cylindrical bar is placed on the centre cradle. Trial instructions are provided on the screen. In the example, the instructions require the subject to place the bar on the right cradle (R), as indicated by the direction cue, and with the black end to the left, as indicated by the goal-orientation cue. In this example a rotation of the bar is required.

participants' posture could either be in a 'start-posture congruent' posture or 'goal-posture congruent' posture with the planned action (because the action involves a rotation, start- and goal-posture are necessarily opposite). During trials requiring 90 degrees bar rotation (VERTICAL ending trials), participants' posture could either be 'start-posture congruent' or 'start-posture incongruent', while always being incongruent with the goal-posture (because we never asked participants to keep their hand in a thumb-up or –down orientation). Conditions are illustrated in Figure 2.
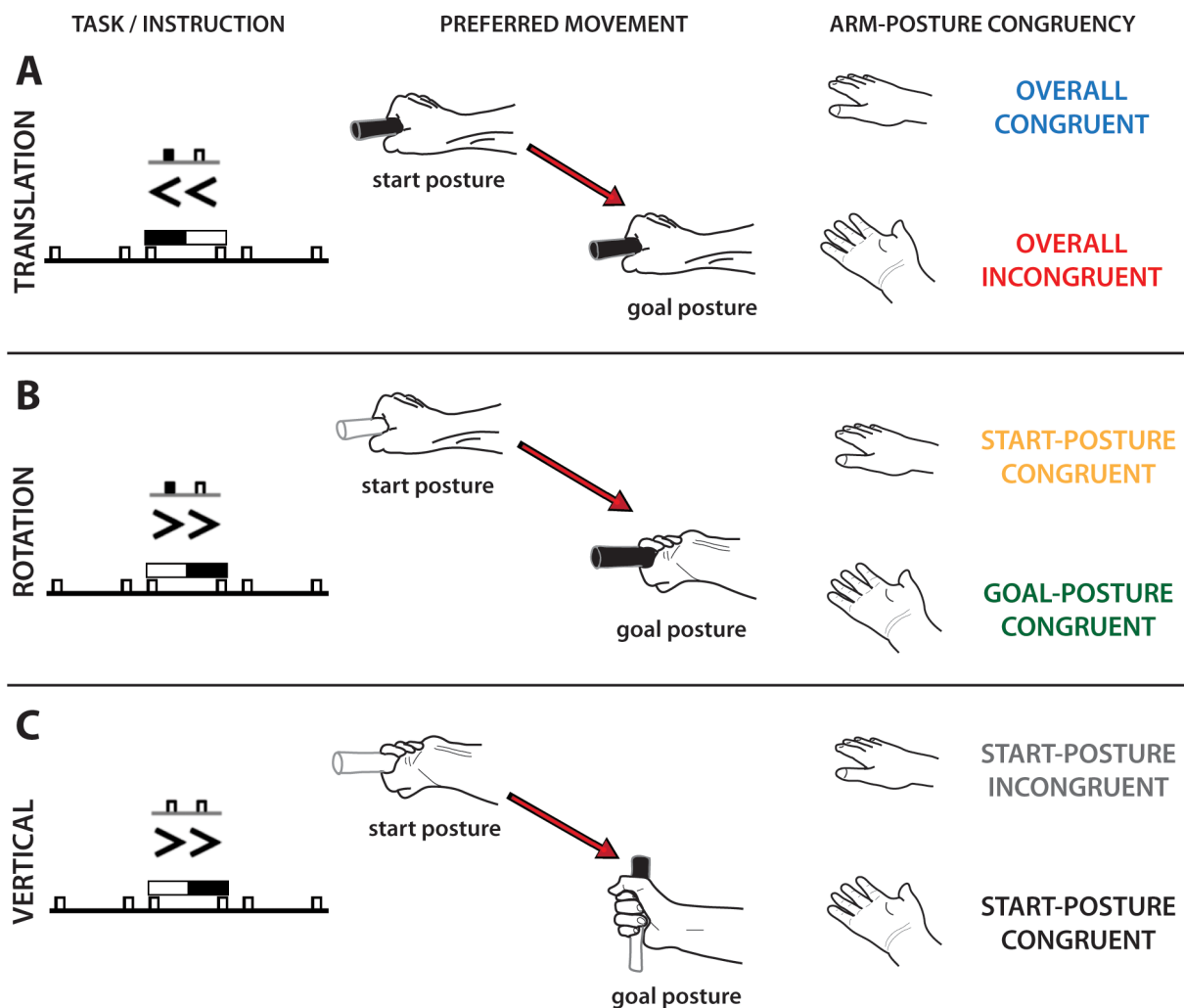
2.3 Experimental procedure

Upon arrival in the lab, we introduced participants to the kinematics lab where we administered the ME task. They were made comfortable with the recording device, we attached sensors required for motion tracking to their wrist, and introduced them to the task. After a short (~5 trials) training participants were able to perform the ME task. They completed 96 trials (32 rotation, 32 no rotation, and 32 vertical trials) in about 20 minutes.

Next, we brought participants to the MRI lab, where they were checked for MR compatibility and introduced to the MP task. They performed 15 practice trials outside the scanner, followed by 40 practice trials inside the scanner (during T1 scanning). The MP task itself consisted of 320 trials (120 no rotation, 120 rotation, 80 vertical), and lasted 45 minutes. We divided the task in two sessions of 25 and 20 minutes. After the experiment participants were debriefed and rewarded. Total lab time of participants, including all preparation phases, was about two hours.

2.4 Behavioral data acquisition

During ME, we measured hand position over

Fig. 2 Motor planning (MP) task. Stimuli and conditions of motor planning (MP) task with translation **(A)**, rotation **(B)** and vertical **(C)** trials. Left column shows example stimuli (compare Figure 1). Middle column shows preferred start- and goal-posture during the movement. Right column shows the participant's possible arm postures, as well as how these result in (in)congruency between body posture and posture(s) of the planned movement.

time using two motion tracking sensors (Polhemus Liberty, sampling frequency: 240 Hz) attached to both sides of participants wrists and saved the data for offline processing and analysis. For preprocessing, we sequenced hand trajectories into different parts on a trial-by-trial basis. The first part was defined as the hand's movement from the resting position until grasping of the bar; the second part as the object transportation until placing at the target; and the remaining part was defined as the return phase, which is of no further interest. For sequencing we combined a predefined target region with a minimum-speed approach. Sequences were divided at the moment when (a) the hand was close to the bar (within box range of 10x5x5 (width, depth, height) cm centered on the cradles), and (b) the hand's velocity was at its lowest within that area. For each trial/movement we retrieved three time points: when a subject starts moving, when he grasps the bar, and finally, when he places it. Additionally, we retrieved hand orientation at the moments of grasping and placing. We based error detection on deviant hand orientation compared to the trial instructions, and removed those trials (on average, 4.2% of the trials were removed by this procedure).

During MP, we used button box responses to establish hand orientation of planned grasping (by combining the response with the instruction about initial bar orientation per trial), and response latencies as movement planning times. Trials with reaction times two standard deviations above a participant's condition mean were removed from analysis (on average, 8.41% of the trials were removed by this procedure).

2.5 Behavioral data analysis

We used Matlab 7.9 for behavioral analyses. First, we compared grip preference and movement/ planning times between tasks to ensure their common grounding on motor control, using a correlation approach. For each condition (target direction, initial orientation, final orientation, and initial posture) we computed average movement and planning times as well as average grip preferences.

We defined grip preference as the ratio underhand grip/trials per condition, leading to values between 0 (always overhand) and 1 (always underhand). We defined planning times as the time required to give a response and movement times as the time to place the bar onto the target cradle. In a further step we computed group means for all conditions over both tasks, which we tested for correlation.

Then, we analyzed reaction times from the MP task for action complexity- and posture-effects. As a measure of the action complexity effect we used the reaction time difference between easy (i.e. NO ROTATION) and difficult (i.e. ROTATION) trials. Posture effects were analyzed for each trial type apart: in NO ROTATION trials a posture effect was defined as the difference in reaction time with an overall congruent and overall incongruent posture; in ROTATION trials posture effect was defined as the reaction time difference between trials where participants own posture reflects the start posture and trials where the own posture reflects the goal posture of the planned movement; in VERTICAL trials posture effect was defined as the reaction time difference between trials where participants own posture does reflect the start posture and trials where it does not.

2.6 Image data acquisition

We used a 1.5 T Avanto MR-scanner (Siemens, Erlangen, Germany) to acquire whole-brain T2*-weighted gradient-echo echo-planar images (TR=2140ms, TE=40 ms 3.5x3.5x3.0 mm voxels, inter-slice gap = 0.5 mm). We used a 32-channel head coil for signal reception. Per participant, a total of about 1400 volumes were collected. The first 5 volumes of each scan were discarded to allow for T1 equilibration effects.

2.7 Imaging data analysis

Imaging data were analyzed using SPM5 (Wellcome Department of Cognitive Neurology, London, UK). For preprocessing, all images were realigned spatially to the first volume, and the signal in each slice was realigned temporally to the first slice using a sinc interpolation.

Resliced volumes were then normalized to a standard EPI template based on the MNI reference brain in Talairach space. The normalized images were smoothed with an 8-mm FWHM isotropic Gaussian kernel. Treating the volumes as a time series, the data were high-pass filtered to 1/128 Hz. Smoothed images were scaled to a grand mean of 100 over all voxels and scans within a session.

Three times two event types were defined: (1) NO ROTATION trials, which were further divided into those with (1a) overall congruent, and (1b) overall incongruent posture; (2) ROTATION trials, which were further divided into those with (2a) start posture congruent, and (2b) goal posture congruent

posture; and (3) VERTICAL ending trials, which were further divided into those with (3a) congruent start posture and (3b) incongruent start posture. Note that for the latter trial type, the own posture and planned end posture are always incongruent.

Each analysis was performed in a two-stage procedure. In the first stage, the BOLD response for each event type was modeled with the canonical HRF and its temporal derivative. These functions were convolved with an event train of short boxcar functions at each stimulus onset, and used to create covariates in a GLM. The length of the Boxcar functions was defined as a participant's average reaction time. Parameter estimates for each covariate were calculated from the least-mean-squares fit of the model to the time series. Images of the parameter estimates for the canonical and derivative covariates were created by subject-specific contrasts (collapsing across sessions within subjects). These "summary statistic" images comprised the data for a second stage of repeated-measures analyses, treating subjects as a random variable. Pairwise one-tailed contrasts on the canonical parameter images allowed t-tests on differences in the magnitude of event-related responses. We included for each participant the effect size as covariate in the analysis of magnitude differences.

Canonical SPMs were thresholded at p < .001. Additionally, analysis was restricted to clusters that were comprised of at least 10 voxels. Regions of interest (ROI) were selected based on previous research. For SPL [-22 -60 58] we used coordinates from de Lange et al. (2006), for EBA [-49 -72 -2] we used coordinates from Downing et al. (2001). Statistics were done on small volume corrected regions of 10 mm spheres around ROIs. Maxima of identified regions were localized as good as possible to the system of Talairach and Tournoux (Talairach and Tournoux, 1988).
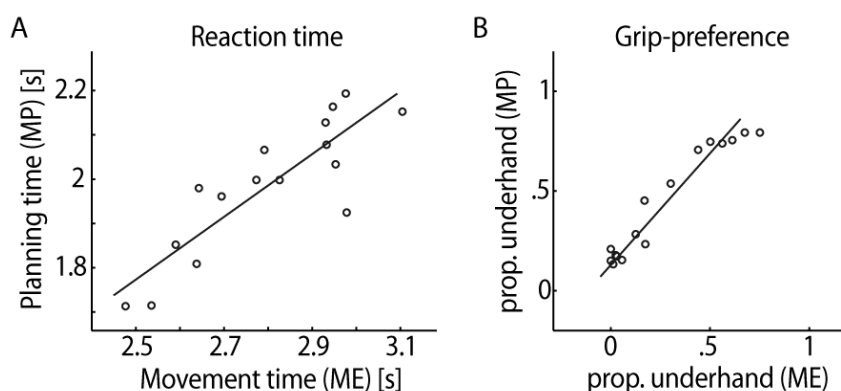
3. Results

3.1 Behavioral Results

3.1.1 Motor execution

We obtained movement time (MT) measures and observed grip preference during the motor execution task. MT was larger for trials that required a rotation of the bar (ROTATION trials) than trials that did not (NO ROTATION trials, see Fig 2 for examples) (difference=418 ms: t=7.299, p<.001). Based on comfort ratings for various postures taken from Rosenbaum (1992) we predicted whether for a particular action sequence in our task participants would prefer an initial over- or underhand grip. Observed preferences during movement execution strongly correlated with predicted grip preferences (r=.941, p<.001), in line with models of end-state comfort.
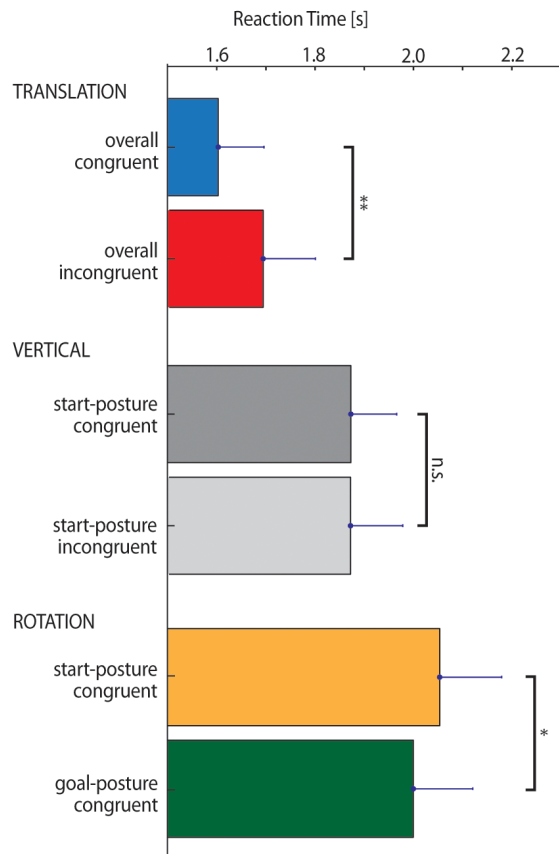
3.1.2 Motor planning

We collected reaction time (RT) measures and indicated grip preference during the motor planning task. In good correspondence with the motor execution task, participants were slower in ROTATION trials than NO ROTATION trials (difference: 383ms, F(1,16)=41.177, p<.001), and when comparing RTs for different action plans with MTs for corresponding action plans, there was a tight correlation between these two (r=.86, p<.001, Figure 3a). Also, indicated grip preference correlated strongly with predicted grip preferences (r=.857, p<.001), and with grip preferences obtained from the ME task (r=.97, p<.001, Figure 3b). Together, these data indicate that the duration and outcome of cognitive processes during the motor planning task are highly similar to those observed during actual

Fig. 3 Comparison of behavioral performance during ME and MP task. Average movement times (**A**), in seconds and grip preference (**B**) proportion underhand grips) during ME for all possible movements are highly similar to average reaction times and preference during MP for corresponding movement types.
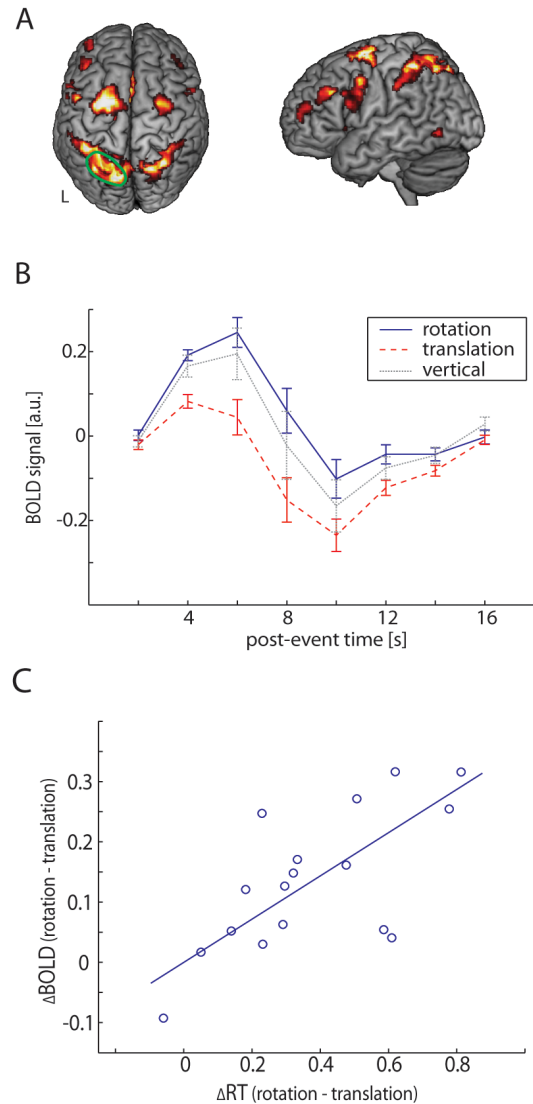
Fig. 4 Behavioral performance during MP task. Plotted are averages of planning times for different movement types (translation, vertical, rotation) as well as effects of posture congruency on each movement type. See Figure 2 for detailed description and color coding of conditions.

motor execution.

3.1.3 Effect of hand posture

We next assessed the effect of hand posture on RT during the motor planning task. During NO ROTATION trials, participants' posture could either be 'overall congruent' or 'overall incongruent' with the planned action (because the start- and goal-posture are the same for these actions, see Figure 2). Participants were faster with their hand in an 'overall congruent' posture than in an 'overall incongruent' posture (difference=93 ms: $F(1,16)=9.916$, p=.006). During ROTATION trials, participants' posture could either be in a 'start-posture congruent' posture or 'goal-posture congruent' posture with the planned action (because the action involves a rotation, start- and goal-posture are necessarily opposite). Here, participants were faster when their hand was in a 'goal-posture congruent' compared to a 'start-posture congruent' posture (difference=54 ms: $F(1,16)=4.713$, p=.045). During VERTICAL ending trials posture manipulation had no effect on
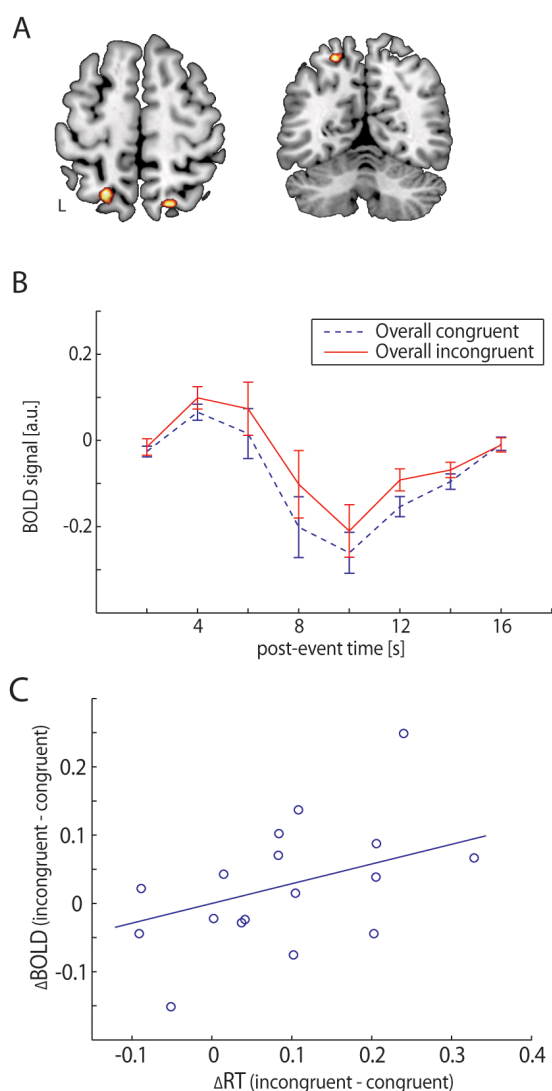

Fig. 5 Neural activity modulated by complexity of movement plan. **(A)** Brain rendering showing areas that were significantly more activated as a function of movement complexity during the MP task (rotation > translation, thresholded at T > 4 for display purposes). **(B)** Event-related response of left IPS (box), plotted for different levels of complexity of the movement plan. **(C)** Correlation between BOLD and RT differences of each subject between rotation and translation trials. For details on conditions and color coding, see Figure 2.

RTs ($F(1,16)=0.002$, n.s.; p=.962), that is, they were equally fast regardless of whether their own posture was congruent or incongruent to the start-posture of the planned movement.

3.2 Neural Activity

3.2.1 Movement complexity

When comparing ROTATION with NO ROTATION trials, we observed increased activity in a network spanning superior parietal, dorsal precentral and inferior frontal cortex (Fig 5A-B). A correlation analysis showed that there was a tight link

Fig. 7 Neural activity modulated by goal-posture congruency. **(A)** Anatomical localization of areas that were more active when body posture was incongruent with the goal posture of the movement plan during the MP task (thresholded at T > 2 for display purposes). **(B)** Event-related response of left EBA, plotted for different levels of body posture congruency. For details on conditions and color coding, see Figure 2.
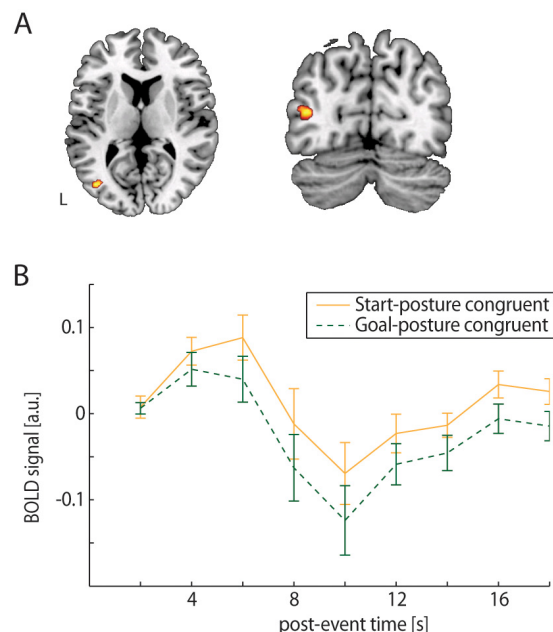

Fig. 6 Neural activity modulated by overall body posture congruency. **(A)** Anatomical localization of areas that were more active when body posture was overall incongruent with the movement plan during the MP task (thresholded at T > 2 for display purposes). **(B)** Event-related response of left IPS, plotted for different levels of body posture congruency. (C) Correlation between BOLD and RT differences of each subject between congruent and incongruent posture. For details on conditions and color coding, see Figure 2.

between inter-subject variability in RT differences between ROTATION and NO ROTATION trials on the one hand and neural activity difference s between these conditions on the other hand in the left superior parietal lobe (r=.682, p<.01). A complete list of activated brain regions can be found in the supplementary materials.

3.2.2 Effect of hand posture

During NO ROTATION trials, we observed increased neural activity in the left and right SPL when subject's hand posture was overall incongruent with the planned action (Figure 6A-

B). Moreover, inter-individual differences in BOLD activity between congruent and incongruent posture conditions correlated with differences in reaction times between postures (Figure 6C: r=.521, p<.05).

During ROTATION trials, neural activity increased when participants adopted a start-posture congruent hand posture (compared to goal-posture congruent hand posture) in the left middle occipital gyrus, falling close to the putative extrastriate body area (EBA: euclidean distance = 7 mm; Downing et al., 2001).

Manipulation of hand posture had no effect on VERTICAL ending trials where participants were instructed to place the bar vertically between a cradle pair, that is, with the own hand posture congruent or incongruent to the start-posture of the movement alone (while always incongruent with the goal-posture). For a summary of all posture effects see Table 1.

4. Discussion

This study investigated how one's own body posture interacts with the planning of goal-directed actions. Behavioral results supported the hypothesis that motor planning is facilitated when one's body state is congruent with the goal-posture of the planned movement. In neural terms, two regions were modulated by body posture: the superior

Table 1. Posture congruency effects during the motor planning task. Activity differences in the areas in bold font are based on an analysis within an a priori search space and survived multiple comparisons correction. Activity differences in the other listed areas were significant at a lenient threshold of p<0.001 uncorrected but did not survive correction for multiple comparisons. Therefore, these areas are solely listed for reference. Cluster size is given in number of voxels.

Contrast	Anatomical region	MNI coordinates			Cluster size	*t*-value
		x	y	z		
Incongruent > congruent overall posture (translation trials)	**Intraparietal sulcus**	-20	-60	58	14	4.39
		20	-68	58	20	4.35
	Precentral gyrus	-10	-24	56	14	4.51
	Inferior frontal gyrus	-38	24	22	13	4.49
	Caudate nucleus	22	26	6	11	5.43
Incongruent > congruent goal posture (rotation trials)	**Middle occipital gyrus (EBA)**	-42	-72	2	54	5.48
	Fusiform gyrus	30	-64	10	17	4.76
	Superior medial gyrus	2	46	46	34	5.99
	Postcentral gyrus	-48	-30	61	13	4.61
	Postcentral gyrus	-62	-12	20	27	4.23
	Postcentral gyrus	66	-22	20	12	3.91

parietal lobe (SPL) and the extrastriate body area (EBA). SPL was more active when the body posture was different from the posture used in a motor plan for translation of an object than when postures were the same. EBA was more active when the body posture was the same as the start-posture used in a motor plan for rotating an object compared to when it was the same as the goal-posture of the same motor plan. Together, our results indicate that movement planning is facilitated (in terms of behavioral performance and neural computation) by adopting the goal posture of the movement. This is in line with models that suppose that movement planning is predicated on the specification of goal postures (Rosenbaum et al., 2001; Graziano et al, 2002).

4.1 Behavioral results - Importance of end-posture in movement planning

When participants decided how to grasp the bar, they predominantly selected the option that had a comfortable end-posture, which suggests that motor planning determines the solution to the selection problem on the basis of the end-state of an action. This is further supported by the observation that planning of movements is facilitated when proprioceptive information about one's body state is congruent with the movement's goal-state. Thereby, our behavioral results support Rosenbaum's theory, that movement planning is organized around goal postures.

4.2 Parietal and premotor cortex are modulated by movement complexity

The motor planning task activated a fronto-parietal network comprising the superior parietal, dorsal precentral and inferior frontal cortex. Activity within this network increased with increasing complexity of the movement plan, from a simple translation to combined translation and rotation movements. The involvement of superior parietal and dorsal precental cortex during the elaboration of motor plans is in line with previous studies of movement planning in humans (Beurze et al., 2007) and monkeys (Kalaska et al., 1997; Scott et al., 1997).

4.3 Body posture interacts with motor planning

There were two regions whose activity was modulated by participant's body posture during the movement planning task: SPL and EBA. Interestingly, both of these have been suggested to contain a body representation (SPL: Wolpert et al., 1998; Ehrsson et al., 2000; EBA: Downing et al., 2001; Astafiev et al., 2004; Saxe et al., 2006; Kuhn et al., in press). In our study, SPL showed increased activity during planning of simple translation movements when one's arm posture was different from the posture used in the motor plan. EBA showed increased activity during planning of more complex rotation movements when one's arm posture was different from the goal posture. In the following section, we will discuss potential functions of both areas during

the generation of a motor plan.

4.3 Body state estimation in posterior parietal cortex

The parietal cortex integrates sensory information from multiple modalities with motor plan information from efference copies (Andersen et al., 1997). These sources of information can be used to generate an estimate of a body state, in order to achieve an optimal representation of the current body state and predict future states (Wolpert and Ghahramani, 2000; Grush, 2004). Our finding of increased activation in the parietal cortex when there was larger incongruence between one's arm posture and the planned arm posture in translation movements is supportive of this idea. The enhanced activation can be related to the larger computational load necessary to merge the proprioceptive body-related information with the motor plan. This is compatible with earlier studies on mental simulation of reaching (de Lange et al., 2006) and grasping movements (Grezes et al., 2003; Vargas et al., 2004).

Surprisingly, SPL was not modulated by body posture when participants planned complex rotation movements. During generation of these motor plans body posture was congruent to either the start- or goal-posture of the planned movement. Absence of activation differences may however be related to the fact that congruent and incongruent phases cancel out each other in these motor plans. That is, if body posture is congruent with the start-posture of the planned movement then we expect low activity when estimating early parts of the motor plan, but high activity when estimating later parts of the motor plan, and vice versa when body posture is congruent with the goal-posture. The temporal difference may be too small to be detected in the slow BOLD signal. Clarification could be given by neuroimaging techniques with high temporal resolution like MEG or EEG.

4.4 Goal-state estimation in EBA

Besides SPL, EBA was modulated by body posture in complex trials that involved rotation of the bar. Originally, EBA has been assumed to be a pure visual area involved in the perception of body parts (Downing et al., 2001). However, later studies showed that EBA is also activated during planning of voluntary manual actions (Kuhn et al., in press), and is involved in representing one's body by combining information from multiple modalities

(Astafiev et al., 2004). Here we observed that EBA is more active during movement planning when one's body posture is incongruent with the goal-posture of a motor plan. This suggests that EBA may contain a visual or multimodal representation of an action's goal-state when a motor plan is generated. This may make EBA a candidate region involved in the selection of an appropriate goal-posture, which results in the earlier mentioned end-state comfort effect. Such a representation of the goal-state may be evaluated in terms of comfort and other aspects.

There are two possibilities how EBA may be involved in motor planning. One possibility is that EBA is involved early during the generation of a motor plan, which is motivated by Kuhn et al. (in press). In a given task, a visual representation of the desired goal-posture may be generated in EBA in visual terms. Subsequently, as assumed in ideomotor theory (Hommel et al., 2001), the visual representation may activate a motor plan that achieves the desired goal-state. Another possibility, motivated by Astafiev et al. (2004), is that a body representation in EBA is updated by efference copies of an earlier generated motor plan (that is, EBA is involved later on during motor planning). This updated body representation may then be evaluated, leading to for example movements that are finished with a comfortable body posture.

However, EBA was not modulated by body posture during the planning of simple translation actions. This lack of modulation may be the result of the fact that overall less computation was required for these simple actions. In a study by Helmich et al. (2007), EBA was increasingly activated with biomechanical complexity of a movement, particularly in Parkinson's disease patients, which may reflect increased reliance on a visual representation of one's body during planning. A study by Dijkerman et al. (2009) gives additional, indirect support for the idea that EBA is especially involved in planning of complex actions. They tested patients with lesions in lateral occipital areas and occipito-parietal and –temporal regions in a task that, even stronger than our task, predicts actions according to the end-state comfort effect. Despite being able to grasp and move objects according to instructions, patients showed abnormal grip behavior in more complex trials. EBA may therefore not be critical for planning, but recruited in order to improve grasping behavior.

4.5 Conscious report of grip orientation

A critical point in this study is that in normal behavior grip selection might be rather automatic and its outcome (such as the arm orientation during grasping) might not be consciously available to the actor. Here, we asked participants to indicate by button press how they would grasp a button, which might interfere with the processes in a way that is not controlled for by contrasting of conditions (i.e. subtraction method). The manipulated factor hand posture may influence the ease with which participants in our study can report their grip orientation. In particular, the adopted hand posture can be congruent or incongruent to the hand orientation inherent to the report participants have to give. For example, when in the initial bar configuration the black part is on the left end, and subjects use an overhand grip, they have to press the button assigned to black. The inherent orientation to grasp the bar such that one's thumb rests on the black end is an overhand (prone) grip orientation. If body posture does effect the ease with which a report is given, we should see facilitation when one's body posture is congruent to the begin state of the planned action. The results however showed the opposite pattern, meaning that it is highly unlikely that the observed goal state facilitation resulted from such interference. Furthermore, such an effect should especially be visible during the VERTICAL condition, where congruency was only manipulated between one's physical body posture and an action's start posture.

5. Conclusions

Behaviorally we observed facilitation of motor planning if one's body posture is congruent to the goal-state (but not its begin-state) of the planned movement. Neurally we observed that SPL and EBA are differentially modulated by one's own body posture during motor planning. From these results we conclude that the SPL maintains an internal representation of one's own body, while a visual representation of a movement's desired goal-state is generated in EBA. The former is probably used to inform motor plans about object properties (Davare et al., 2010), and the latter one may be used to improve our behavior in characteristics that are not directly linked to the success of actions.

From the behavioral results as well as activation differences in SPL and EBA we conclude that motor planning is organized around goal postures rather than discrete limb or joint movements. Moreover, we can conclude that one's body posture is relevant in the generation of motor plans, which emphasizes the embodied nature of motor planning.

Acknowledgements

References

Alexander RM (1997) A minimum energy cost hypothesis for human arm trajectories. Biol Cybern 76:97-105.

Andersen RA, Snyder LH, Bradley DC, Xing J (1997) Multimodal representation of space in the posterior parietal cortex and its use in planning movements. AnnuRevNeurosci 20:303-330.

Astafiev SV, Stanley CM, Shulman GL, Corbetta M (2004) Extrastriate body area in human occipital cortex responds to the performance of motor actions. Nat Neurosci 7:542-548.

Bernstein N (1967) The coordination and regulation of movements. London: Pergamon.

Beurze SM, de Lange FP, Toni I, Medendorp WP (2007) Integration of target and effector information in the human brain during reach planning. JNeurophysiol 97:188-199.

Davare M, Rothwell JC, Lemon RN (2010) Causal connectivity between the human anterior intraparietal area and premotor cortex during grasp. Curr Biol 20:176-181.

de Lange FP, Helmich RC, Toni I (2006) Posture influences motor imagery: an fMRI study. Neuroimage 33:609-617.

Dijkerman HC, McIntosh RD, Schindler I, Nijboer TC, Milner AD (2009) Choosing between alternative wrist postures: action planning needs perception. Neuropsychologia 47:1476-1482.

Downing PE, Jiang Y, Shuman M, Kanwisher N (2001) A Cortical Area Selective for Visual Processing of the Human Body. Science 293:2470-2473.

Ehrsson HH, Naito E, Geyer S, Amunts K, Zilles K, Forssberg H, Roland PE (2000) Simultaneous movements of upper and lower limbs are coordinated by motor representations that are shared by both limbs: a PET study. Eur J Neurosci 12:3385-3398.

Flash T, Hogan N (1985) The coordination of arm movements: an experimentally confirmed mathematical model. J Neurosci 5:1688-1703.

Grafton ST, Hamilton AF (2007) Evidence for a distributed hierarchy of action representation in the brain. Hum Mov Sci 26:590-616.

Graziano MS, Taylor CS, Moore T (2002) Complex movements evoked by microstimulation of precentral cortex. Neuron 34:841-851.

Grezes J, Tucker M, Armony J, Ellis R, Passingham RE (2003) Objects automatically potentiate action: an fMRI study of implicit processing. EurJ Neurosci 17:2735-2740.

Grush R (2004) The emulation theory of representation: motor control, imagery, and perception. BehavBrain Sci 27:377-396.

Helmich RC, de Lange FP, Bloem BR, Toni I (2007) Cerebral compensation during motor imagery in Parkinson's disease. Neuropsychologia 45:2201-2215.

Herbort O, Butz MV (2010) Planning and control of hand orientation in grasping movements. Exp Brain Res 202:867-878.

Hommel B, Musseler J, Aschersleben G, Prinz W (2001) The Theory of Event Coding (TEC): a framework for perception and action planning. BehavBrain Sci 24:849-878.

Kalaska JF, Scott SH, Cisek P, Sergio LE (1997) Cortical control of reaching movements. CurrOpinNeurobiol 7:849-859.

Kording KP, Wolpert DM (2006) Bayesian decision theory in sensorimotor control. Trends Cogn Sci 10:319-326.

Kuhn S, Keizer AW, Rombouts SA, Hommel B (in press) The Functional and Neural Mechanism of Action Preparation: Roles of EBA and FFA in Voluntary Action Control. J Cogn Neurosci.

Rosenbaum DA, Vaughan J, Barnes HJ, Jorgensen MJ (1992) Time course of movement planning: selection of handgrips for object manipulation. J Exp Psychol Learn Mem Cogn 18:1058-1073.

Rosenbaum DA, Meulenbroek RJ, Vaughan J, Jansen C (2001) Posture-based motion planning: applications to grasping. Psychol Rev 108:709-734.

Rosenbaum DA, Loukopoulos LD, Meulenbroek RG, Vaughan J, Engelbrecht SE (1995) Planning reaches by evaluating stored postures. PsycholRev 102:28-67.

Rosenbaum DA, Cohen RG, Dawson AM, Jax SA, Meulenbroek RG, van der Wel R, Vaughan J (2009) The posture-based motion planning framework: new findings related to object manipulation, moving around obstacles, moving in three spatial dimensions, and haptic tracking. Adv Exp Med Biol 629:485-497.

Saxe R, Jamal N, Powell L (2006) My body or yours? The effect of visual perspective on cortical body representations. Cereb Cortex 16:178-182.

Scott SH, Sergio LE, Kalaska JF (1997) Reaching movements with similar hand paths but different arm orientations. II. Activity of individual cells in dorsal premotor cortex and parietal area 5. JNeurophysiol 78:2413-2426.

Sirigu A, Duhamel JR (2001) Motor and visual imagery as two complementary but neurally dissociable mental processes. J Cogn Neurosci 13:910-919.

Talairach J, Tournoux P (1988) Co-planar stereotaxic atlas of the human brain :3-dimensional proportional system : an approach to medical cerebral imaging. Stuttgart: Thieme.

Vargas CD, Olivier E, Craighero L, Fadiga L, Duhamel JR, Sirigu A (2004) The Influence of Hand Posture on Corticospinal Excitability during Motor Imagery: A Transcranial Magnetic Stimulation Study. CerebCortex.

Wolpert DM, Ghahramani Z (2000) Computational principles of movement neuroscience. NatNeurosci 3:1212-1217.

Wolpert DM, Goodbody SJ, Husain M (1998) Maintaining internal representations: the role of the human superior parietal lobe. NatNeurosci 1:529-533.

Institutes associated with the Master's Programme in Cognitive Neuroscience

Donders Institute for Brain, Cognition
and Behaviour:
Centre for Cognitive Neuroimaging
Kapittelweg 29
6525 EN Nijmegen

P.O. Box 9101
6500 HB Nijmegen
www.ru.nl/neuroimaging/

Donders Institute for Brain, Cognition
and Behaviour:
Centre for Neuroscience
Geert Grooteplein Noord 21, hp 126
6525 EZ Nijmegen

P.O. Box 9101
6500 HE Nijmegen
www.ru.nl/neuroscience

Donders Institute for Brain, Cognition
and Behaviour:
Centre for Cognition
Montessorilaan 3
6525 HR Nijmegen

P.O. Box 9104
6500 HB Nijmegen
www.ru.nl/cognition/

Max Planck Institute for Psycholinguistics
Wundtlaan 1
6525 XD Nijmegen

P.O. Box 310
6500 AH Nijmegen
http://www.mpi.nl

MAX-PLANCK-GESELLSCHAFT

Nijmegen Centre for Molecular Life Sciences
Geert Grooteplein 28
6525 GA Nijmegen

P.O. Box 9101
6500 HB Nijmegen
http://www.ncmls.nl

IN·DEI·NOMINE·FELICITER

Universitair Medisch Centrum St Radboud
Geert Grooteplein-Zuid 10
6525 GA Nijmegen

P.O. Box 9101
6500 HB Nijmegen
http://www.umcn.nl/

Baby Research Center
Montessorilaan 10
6525 HD Nijmegen

P.O. Box 9101
6500 HB Nijmegen
http://babyresearchcenter.nl